Chapter 3

Biological Studies of Colorectal Cell Lines

3.1 Introduction

As explained in chapter 1, the aim of this project was to develop a systems biology approach to the analysis and integration of varied biological data from investigations of the anti-tumour activity of RHPS4. Initial studies of this molecule have suggested the mechanism of action involves telomerase inhibition at the sub micromolar level and is possibly linked to its selectivity for G-quadruplex DNA (Cookson *et al*, 2005). It has also been suggested that the mechanism of action of RHPS4 involves cell cycle mediated effects. The aim was to develop a mathematical model to resolve this that was of adequate complexity that the biological results of the laboratory are reproduced, and yet of sufficient simplicity to yield predictive information regarding the possible mechanism(s) of action of RHPS4. Parameterisation of the mathematical models requires robust data from a well-characterised cell line. By robust we mean the ability to give reliable, reproducible, high-quality data regarding both short-term and long-term effects of RHPS4 and other anti-tumour agents on the cell cycle, growth rate and senescence levels of colorectal cancer cell lines.

3.2 Selection of Colorectal Cell Lines

There were four colorectal cell lines chosen for initial study to link with an EPSRC funded project in escience. This was an integrative biology project and the aim was to build a multi-scale computational model of colorectal cancer. The initial studies looked at the HCT116, HT-29, KM12 and HCC-2998 colorectal cell lines.

From this selection of colorectal cell lines the aim was to find a cell line which fulfilled the following criteria:

1. Good growth characteristics in both the presence and absence of RHPS4, and other anti-tumour agents. It was preferable that the cell line chosen would have a flat morphology and would grow in a monolayer type fashion. The reason for this is that in order to analyse the levels of senescence under normal conditions and in response to anti-tumour agents, the preferable method is the staining for SA-β-gal.

2. Good sensitivity to RHPS4 and other anti-tumour agents. It is required that the cells display a good response to RHPS4 and other anti-tumour agents within a good range of concentrations without causing cell death.

3. Tractability in biological assays such as MTT assay and basic cell cycle analysis. In terms of the experiments, it is preferable that the cells are able to be manipulated in a series of experiments in order to define the effects of RHPS4 and other anti-tumour agents.

All four of the colorectal cell lines chosen for initial study were originally isolated from the large intestine. The HCT116 cell line is one of 3 strains of malignant cells which were isolated from a male with colonic carcinoma. In nude mice the cells are tumourigenic and also grow in a monolayer fashion (Brattain *et al*, 1981). Of the 4 cell lines chosen for initial study, HCT116 cells were the only ones which express wild-type p53.

The HT-29 cell line was initially isolated by Fogh & Trempe from a 44-year old Caucasian female with grade II colon adenocarcinoma (Leibovitz *et al*, 1976). The KM12 and HCC-2998 cell line are the least characterized of the four cell lines. It is known, however, that KM12 cells were isolated from a Dukes' B2-stage tumour (Morikawa *et al*, 1988).

Initially, the cells were analysed using the MTT assay to determine their GI_{50} values in response to RHPS4. Following the determination of GI_{50} values, the cells were then incubated with a range of concentrations of RHPS4 based on their GI_{50} values for between 24 and 120 hours to analyse the short-term cell cycle

effects of RHPS4. In order to determine the long-term effects of RHPS4 the cells were analysed at days 4, 6, 10, 14 and 21 for their growth rate, cell cycle and senescence. Based on these results, it was decided which cell line would be used to derive the mathematical model and whose data would be applied to this model.

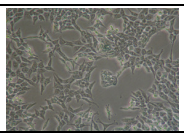
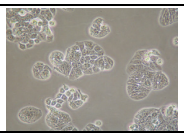
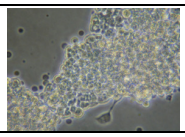
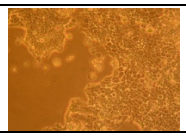
3.2.1 Growth Characteristics

The cells were harvested as in section 2.2.3 and maintained at an approximate confluence of 70% in order for the cells to remain in logarithmic growth phase. Each of the cell lines were observed to determine morphology and approximate doubling times. Observation of the HCT116, HT-29 and HCC-2998 cell lines revealed that they grew in a monolayer fashion, however, the KM12 cell line did not. For the cells to grow in a monolayer fashion is an advantage as senescence analysis is made easier as the most commonly used method to analyse senescence is the SA-β-gal stain. Following staining, the proportion of senescent cells within the population is determined by a simple counting method and when the cells are in a monolayer the counting method is easier, if the cells grow in a similar manner to the KM12 cell line, i.e. in 'clumps', then calculating senescent population is more difficult as it is almost impossible to determine the proportion of senescent cells at the core and beneath the top layer of cells.

The doubling time of each cell line was observed. The HCT116 and HT-29 cell lines had the shortest doubling time of approximately 17 and 19 hours, respectively. The KM12 cell line had a slightly longer doubling time of approximately 24 hours, whilst the HCC-2998 cell line had the longest doubling time of approximately 32 hours. A shorter doubling time is preferable as it is considered that the more doublings the cells go through during the experiment, the more able RHPS4 is to manifest its effects and therefore allow a deeper insight into this complex molecule.

General observations made regarding the cell lines are summarized in table 3.1.

Table 3.1 Observed characteristics of each of the four colorectal cell lines chosen for initial study.

	HCT116	**HT-29**	**KM12**	**HCC-2998**
Morphology				
Doubling time (hours)	17	19	24	32
p53 status	Wild-type	Mutant	Mutant	Mutant

3.2.2 Short-Term MTT Assay to Determine GI_{50} Values

To explore the short-term effects on the viability of the colorectal cell lines in response to RHPS4, MTT assays were carried out using a range of concentrations of RHPS4 and incubation times between 24 and 72 hours. The MTT assay was developed by Mosmann in 1983 and is a colorimetric assay used to detect living, but not dead cells. The signal generated is dependent on the degree of activation of the cells and can therefore be used to measure cytotoxicity, proliferation or activation. The results are read on a multiwell scanning spectrophotometer (ELISA reader) and show a high degree of precision (Mosmann, 1983). The cells were seeded into 96-well plates as in section 2.2.6 and were incubated for up to 72 hours in a range of concentrations of RHPS4. Following incubation, MTT was added to the wells and allowed to metabolise for 4 hours at 37 °C after which the formazan crystals were dissolved in DMSO-glycine buffer and the absorbencies were read at 550 nm. Dose-response curves were produced as shown in figures (3.1) – (3.4) from which the GI_{50}, GI_{25} and GI_{75} values were calculated based on an average of at least 5 repeated assays. As explained in chapter 2, the MTT assays are carried out in 96-well plates meaning that for each concentration of RHPS4 analysed, there are up to 8 repeats within one assay meaning that although the assays are repeated 5 times, the actual number of repeats is a minimum of 40. All four colorectal cell lines displayed good sensitivity to RHPS4, however, to differing degrees. There is a dose-dependent decrease in cell viability as the concentration of RHPS4 increases and is consistent throughout the cell lines. The time-dependent activity is more complex and is discussed below.

Table 3.2 Concentration of RHPS4 causing 25%, 50% and 75% growth inhibition in a panel of four colorectal cell lines

Cell Line	[1]GI_{25}±SD (units stated)		[1]GI_{50}±SD (units stated)		[1]GI_{75}±SD (units stated)	
	24 hour	**72 hour**	**24 hour**	**72 hour**	**24 hour**	**72 hour**
HCT116	**0.1 µM** ±0.1 µM	**0.09 µM** ±0.1µM	**1.0 µM** ±0.4 µM	**0.8 µM** ± 0.7µM	**2.02 µM** ±1.1 µM	**1.09 µM** ±0.7 µM
HT-29	**0.07 µM** ±0.1 µM	**0.009 µM** ±0.005 µM	**0.172 µM** ±0.2 µM	**0.0282µM** ±0.03µM	**0.274 µM** ±0.4 µM	**1.0045 µM** ±1.6 µM
KM12	**0.4 nM** ±0.09 nM	**1.7 nM** ±2.3 nM	**0.7 nM** ±0.2 nM	**3.09nM** ±3.9nM	**2.7 nM** ±1.9 nM	**19.02 nM** ±15.7 nM
HCC-2998			**0.16 µM** ±0.3 µM	**0.18 µM** ±0.3µM		

[1]GI_{25}, GI_{50} and GI_{75} concentration causing 25%, 50% and 75% inhibition, respectively of control cell growth after 24 and 72 hours. The cells were seeded into 96-well plates (for method see section 2.2.6) in culture medium. The cells were allowed to attach overnight and subsequently treated with a range of RHPS4 concentrations at least in quadruplicate. After 24 and 72 hours incubation at 37°C with a 5% CO_2 atmosphere, the MTT assay was carried out to determine cell viability relative to control cells in untreated wells. The values shown are the mean +/- standard deviation of 5 and 7 independent experiments carried out at 24 and 72 hour, respectively.

3.2.2.1 HCT116

The dose response curves of RHPS4 on HCT116 cells are shown in figure 3.1 and show the effects of RHPS4 in a range of concentrations between 0 - 0.1 mM. From these dose-response curves, it is evident that the GI_{50} of RHPS4 on HCT116 cells is 1 µM. There is no significant difference between the GI_{50} at 72 hours from that calculated at 24 hours. The dose response curves at 24 and 72 hours are shown in figure 3.1 and display a dose-dependent reduction in cell viability as the concentration of RHPS4 increases at the two time points, as was expected. At 24 hours, there is a very gradual decrease in cell viability of HCT116 cells in response to the lower concentrations of RHPS4 used with cell death occurring when a concentration of 30 µM RHPS4 is achieved. At 72 hours, the dose response curves shows that HCT116 cells are slightly more sensitive to RHPS4 as there is a rapid reduction in cell viability at the lower concentration in comparison to the dose response curve at 24 hours. Between concentrations of 0.1 µM and 100 µM, the most rapid decline in cell viability is displayed, with cell death occurring at concentrations between 10 µM and 100 µM RHPS4.

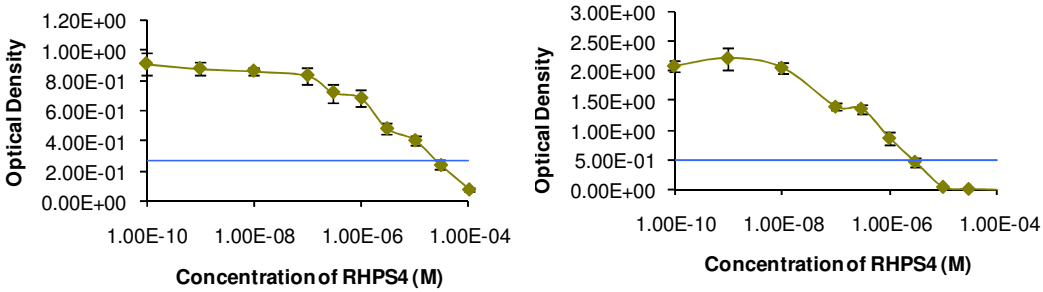


Figure 3.1 Dose response curve for HCT116 at (a) 24 hour and (b) 72 hour obtained from the MTT assay. Each of the graphs shows a representative result of one of 5 at 24 hours and one of 7 at 72 hours. The absorbance values shown are the mean±SD of four replicate wells. The method employed to obtain the above results is shown in section 2.2.6. To obtain a t0 absorbance, i.e. the baseline absorbance value before the addition of RHPS4, an MTT assay was carried out on an additional 96-well plate. Viable cells which are therefore metabolically competent are able to convert MTT to a formazan product which is UV-absorbent upon dissolution with DMSO-glycine (Mosmann, 1983).

3.2.2.2 HT-29

The HT-29 cell line also displayed sensitivity to RHPS4 and according to the MTT assays carried out, had a GI_{50} value of 0.172 μM at 24 hours which changes by a factor of 5 to 0.028 μM by 72 hours. As with HCT116 cells, HT-29 cells displayed a dose-dependent decrease in cell viability as the concentration of RHPS4 increased. The dose-response curves for HT-29 cells to RHPS4 are shown in figure 3.2 and are representative of a minimum of 5 repeats. At 24 hours, there is a slight decline in cell viability between concentrations of RHPS4 of 0 (control) and 1μM, after which there is a rapid reduction in cell viability with cell death occurring at approximately 10 μM. At 72 hours, there appears to be a slight increase in cell viability when 1 nM RHPS4 well concentration is achieved followed by a more rapid decline in cell viability than that seen at 24 hours. At 72 hours, cell death also occurs between concentrations of 10 μM – 100 μM RHPS4.

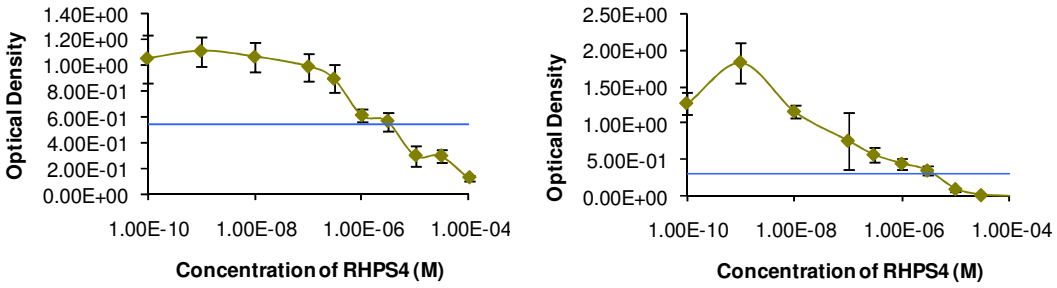


Figure 3.2 Dose response curve for HT-29 at (a) 24 hour and (b) 72 hour obtained from the MTT assay. Again, each of the graphs shows a representative result of one of 5 at 24 hours and one of 7 at 72 hours. The absorbance values shown are the mean±SD of four replicate wells. The method employed to obtain the above results is shown in section 2.2.6. To obtain a t0 absorbance, i.e. the baseline absorbance values before the addition of RHPS4, prior to drug addition, an MTT assay was carried out on a separately prepared 96-well plate. Viable cells which are therefore metabolically competent are able to convert MTT to a formazan product which is UV-absorbent upon dissolution with DMSO-glycine (Mosmann, 1983).

3.2.2.3 KM12

Of all the cell lines, according to the MTT assay, KM12 cells are the most sensitive to RHPS4 with a GI_{50} value of 0.7 nM at 24 hours, rising slightly to 3.1 nM by 72 hours. At 24 hours, the dose-response curves, as shown in figure 3.3, show that there is a rapid decline in cell viability at the lower concentrations of RHPS4 (between 1 nM – 0.3 μM), after which there is a slight increase in cell viability until 1 μM after which there is another rapid decline. The increase in cell viability is a characteristic of the dose-response curves for KM12 cells in response to RHPS4. At 72 hours, this characteristic is lost and there is a steady reduction in cell viability with increasing concentration of RHPS4. The dose-response curves shown in figure 3.3 are typical dose-response curves of KM12 cell in response to RHPS4 and GI_{50} values are calculated from a minimum of 5 repeat experiments.

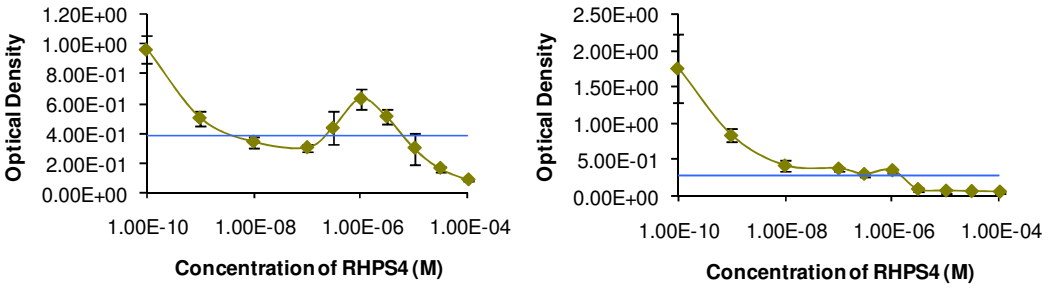


Figure 3.3 Dose response curve for KM12 at (a) 24 hour and (b) 72 hour obtained from the MTT assay. Each of the graphs shows a representative result of one of 5 at 24 hours and one of 7 at 72 hours. The absorbance values shown are the mean±SD of four replicate wells. The method employed to obtain the above results is shown in section 2.2.6. To obtain a t0 absorbance, i.e. the baseline absorbance values before the addition of RHPS4, prior to drug addition, an MTT assay was carried out on a separately prepared 96-well plate. Viable cells which are therefore metabolically competent are able to convert MTT to a formazan product which is UV-absorbent upon dissolution with DMSO-glycine (Mosmann, 1983).

3.2.2.4 HCC-2998

Of all the cell lines, the results of HCC-2998 cells were the most irreproducible; however, they do show similar properties to the other cell lines. HCC-2998 cells display a concentration-dependent decrease in optical density and at 24 hours gradually declines until a concentration of $3x10^{-6}$ M after which, as the concentration increases, cell death occurs. At 72 hours, the optical density declines gradually until a concentration of 1 μM, after which cell death occurs. As with the other cell lines, the sensitivity of the HCC-2998 cells decreases between 24 and 72 hours, again evident from the GI_{50} values. Between 24 and 72 hours, the GI_{50} value increases from 0.158 μM±0.29 μM to 0.179 μM ±0.33 μM.

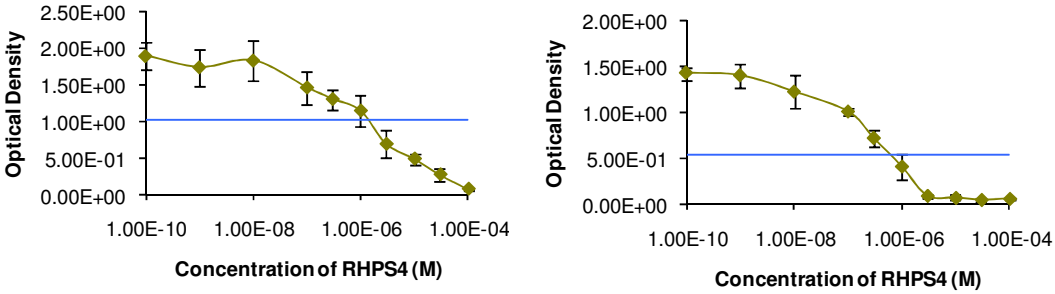


Figure 3.4 Dose response curve for HCC-2998 at (a) 24 hour and (b) 72 hour obtained from the MTT assay. Each of the graphs shows a representative result of one of 5 at 24 hours and one of 7 at 72 hours. The absorbance values shown are the mean±SD of four replicate wells. The method employed to obtain the above results is shown in section 2.2.6. To obtain a t0 absorbance, i.e. the baseline absorbance values before the addition of RHPS4, prior to drug addition, an MTT assay was carried out on a separately prepared 96-well plate. Viable cells which are therefore metabolically competent are able to convert MTT to a formazan product which is UV-absorbent upon dissolution with DMSO-glycine (Mosmann, 1983).

3.2.3 Short-Term Cell Cycle Responses to RHPS4

The cell cycle of each cell line under normal conditions and in response to RHPS4 were analysed using the Nicoletti method as stated in section 2.2.7.1. Based on the GI_{50} values, the cells were incubated for up to 24 hours in media (control), 100 nM, 1 μM and 10 μM RHPS4. The cells were analysed at 1, 3, 6, 16 and 24 hours to determine the short-term effects of RHPS4. Typical cell cycle profiles of control cells of each of the four colorectal cells lines are shown in figure 3.5.

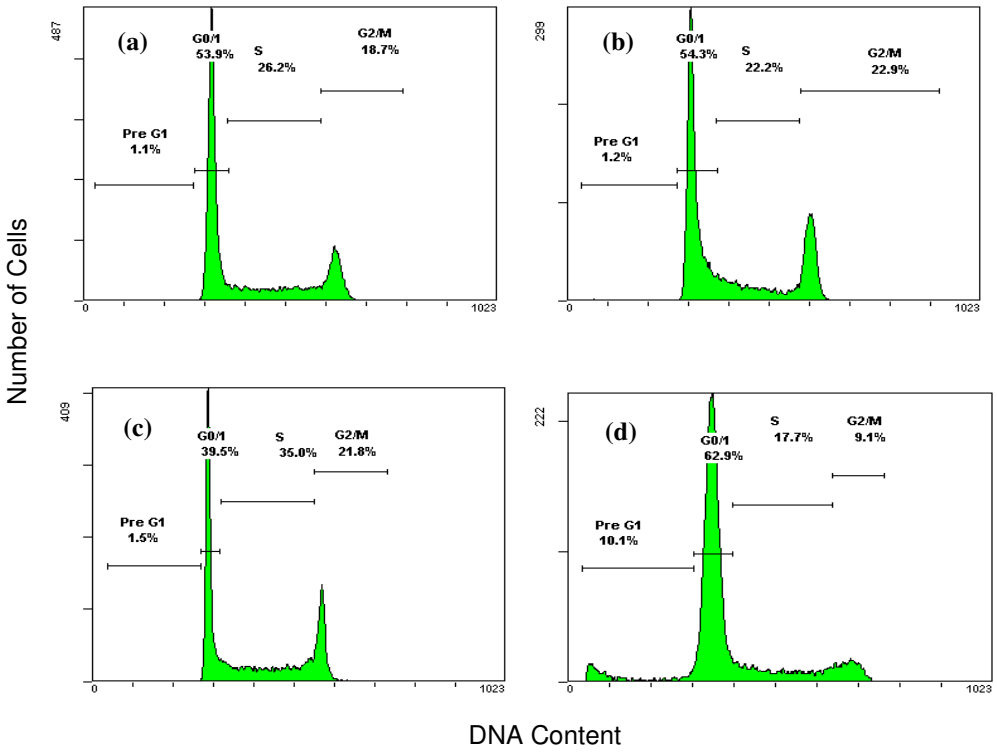


Figure 3.5 Cell cycle profiles of control (a) HCT116, (b) HT-29, (c) KM12 and (d) HCC-2998 cells. Typical cell cycle profiles of the selected colorectal cell lines under normal conditions. Cells were allowed to grow until they reached a confluence of 70% in RPMI medium containing 10% FBS at 37 °C in a 5% CO_2 humidified environment.

3.2.3.1 HCT116

RHPS4 had very little effect on the cell cycle of HCT116 cells up to 24 hours. Figure 3.6 shows representative DNA content histograms of HCT116 at incubation times of 1, 3, 6, 16 and 24 hours in 100 nM, 1 μM or 10 μM RHPS4. There appears to be very little change in the cell cycle distribution at a concentration of RHPS4 of 1 μM. Up to 16 hours, incubation with 10 μM RHPS4 has no significant effect on the cell cycle distribution; however, at 16 hours the proportion of cells in S phase is reduced to approximately 14% from 22%, followed by a further reduction to 9% by 24 hours. This is evident in figure 3.6 and can also be seen in the DNA histograms shown in figure 3.7 There is an increase in the proportion of cells in pre-G_1 at 24 hours when incubated with 10 μM RHPS4 from that of the control, and so this is a potentially toxic concentration. From figures 3.6 – 3.7, it is also apparent that there are no significant changes in the proportion

of cells in G_1/G_0 or G_2/M from that of the control up to 24 hours. In summary, the cell cycle effects of RHPS4 at lower concentrations on HCT116 cells do not become apparent until after 24 hours.

It is also evident from figure 3.7 that RHPS4 causes S phase emptying in HCT116 cells that is not evident in figures 3.9, 3.11 or 3.13 which correspond to the effects of RHPS4 up to 24 hours in HT-29, KM12 and HCC-2998 cells, respectively.

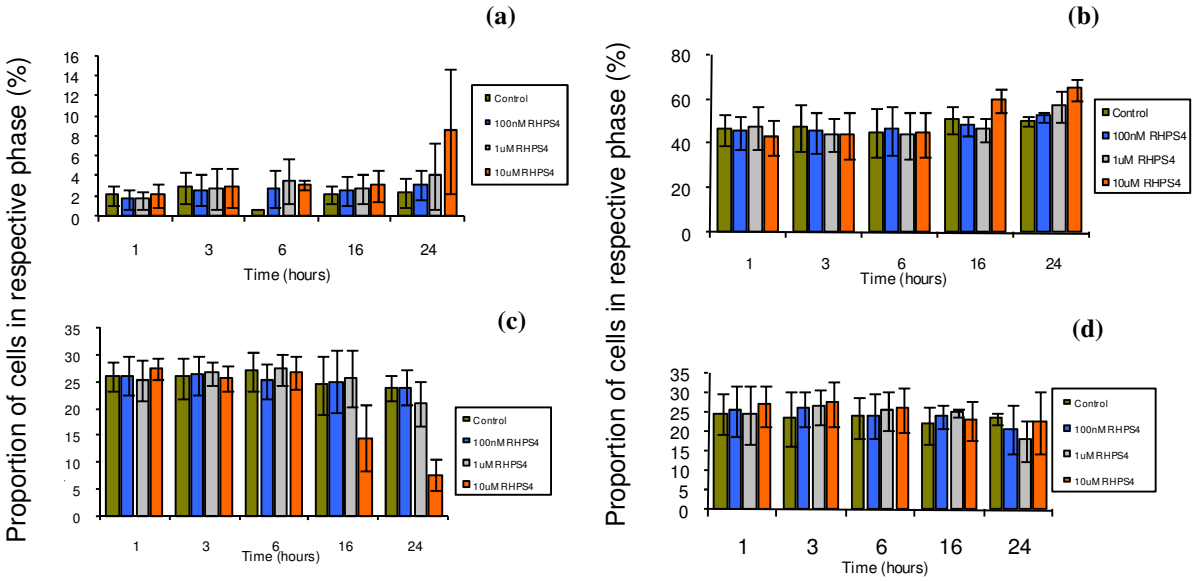


Figure 3.6 Short-term cell cycle distributions of HCT116 cells in response to RHPS4. The cells were incubated with RHPS4 at a range of concentrations up to 24 hours. The cell cycle was analysed using PI which penetrates the nucleus and intercalates with DNA. The cells were then analysed on the Beckman Coulter flow cytometer where 20 000 events were collected and their cell cycles analysed to determine the proportion of cells in (a) pre-G_1, (b) G_1/G_0, (c) S and (d) G_2/M. The graphs shown here are the average ±SD of at least 3 experimental repeats.

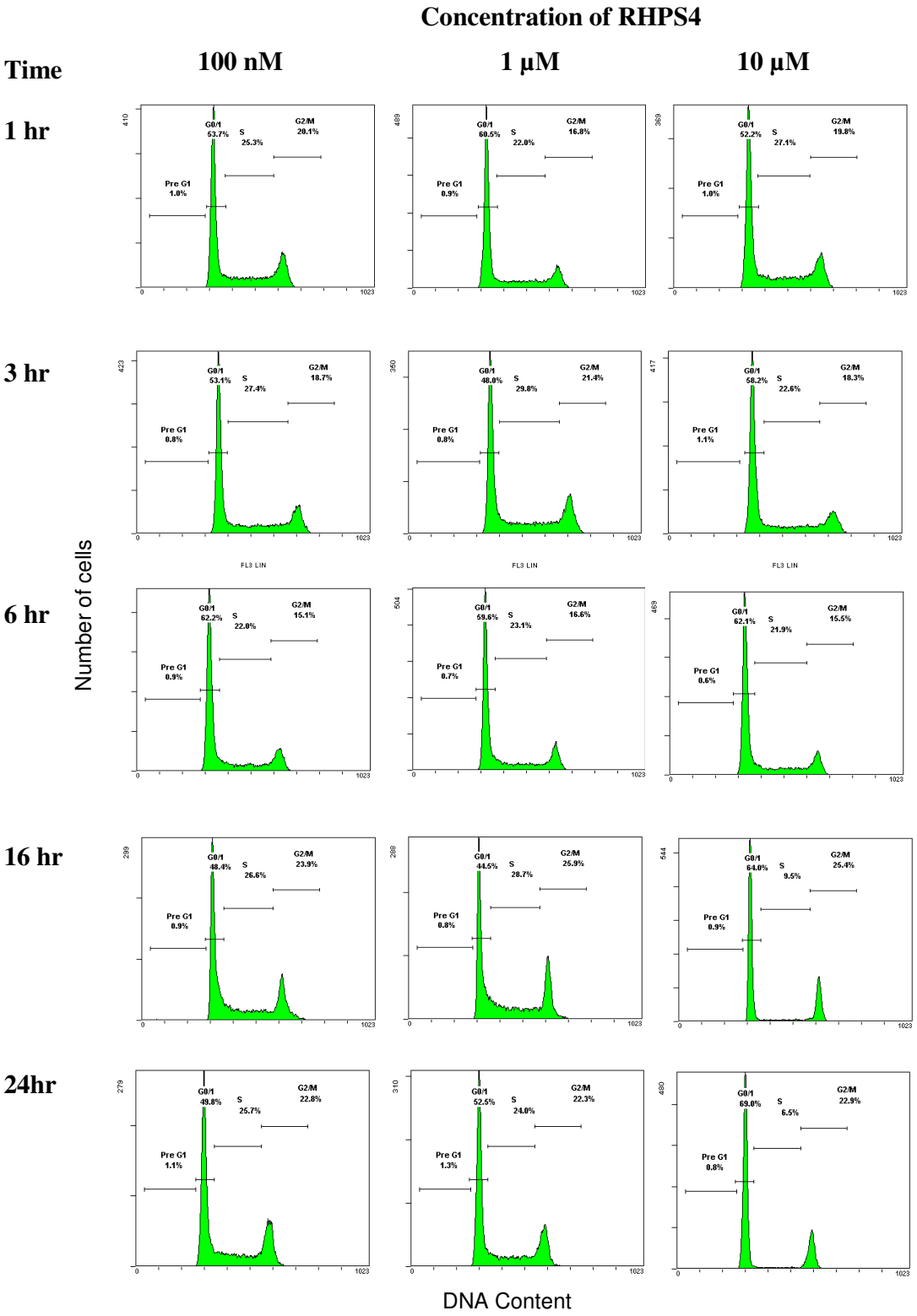


Figure 3.7 Cell cycle distributions of the short-term effects of RHPS4 on HCT116 cells up to 24 hours at 100 nM, 1 µM and 10 µM. The cells were collected as in section 2.2.7.1 using PI and analysed using flow cytometry measuring 20 000 events.

3.2.3.2 HT-29

As with HCT116 cells, there appears to be no significant changes in cell cycle distribution in comparison to control following incubation with RHPS4 up to 24 hours. Graphs of the effects of RHPS4 on each phase of the cell cycle up to 24 hours are shown in figure 3.8 and typical DNA content histograms from which the data is generated are shown in figure 3.9. From figures 3.8 – 3.9, it is evident that there are no significant changes in the proportion of cells in either cell cycle phase with increasing concentration of RHPS4 or time. The proportion of cells in S and G_2/M in particular do not change from that of the control.

The histograms shown in figure 3.9 appear to show change in the proportions of cells in G_2/M, however, the graphs below do not reflect this. The reason for this is the histograms in figure 3.8 are one example of an experiment, whereas the graphs shown in figure 3.9 are the averages of all the experiments carried out.

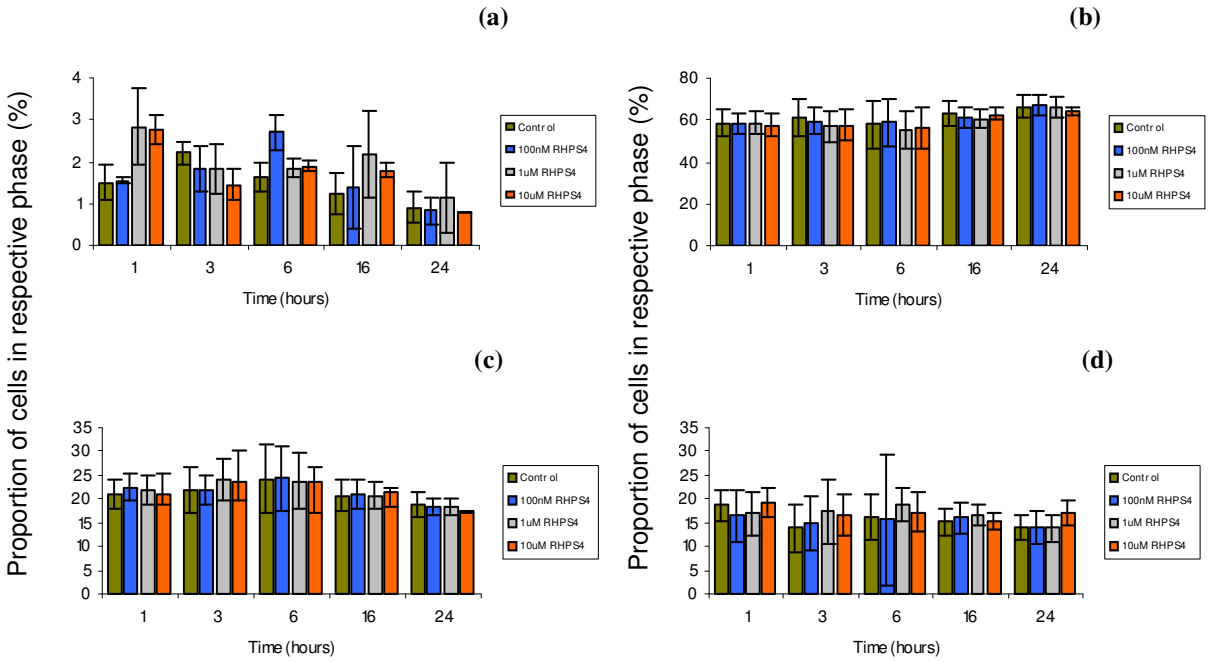


Figure 3.8 Short-term cell cycle distributions of HT-29 cells in response to RHPS4. The cells were incubated with RHPS4 at a range of concentrations up to 24 hours. The cell cycle was analysed using PI which penetrates the nucleus and intercalates with DNA. The cells were then analysed on the Beckman Coulter flow cytometer where 20 000 events were collected to determine the proportion of cells in (a) pre-G_1, (b) G_1/G_0, (c) S and (d) G_2/M. The graphs shown here are the average (±SD) of at least 3 experimental repeats.

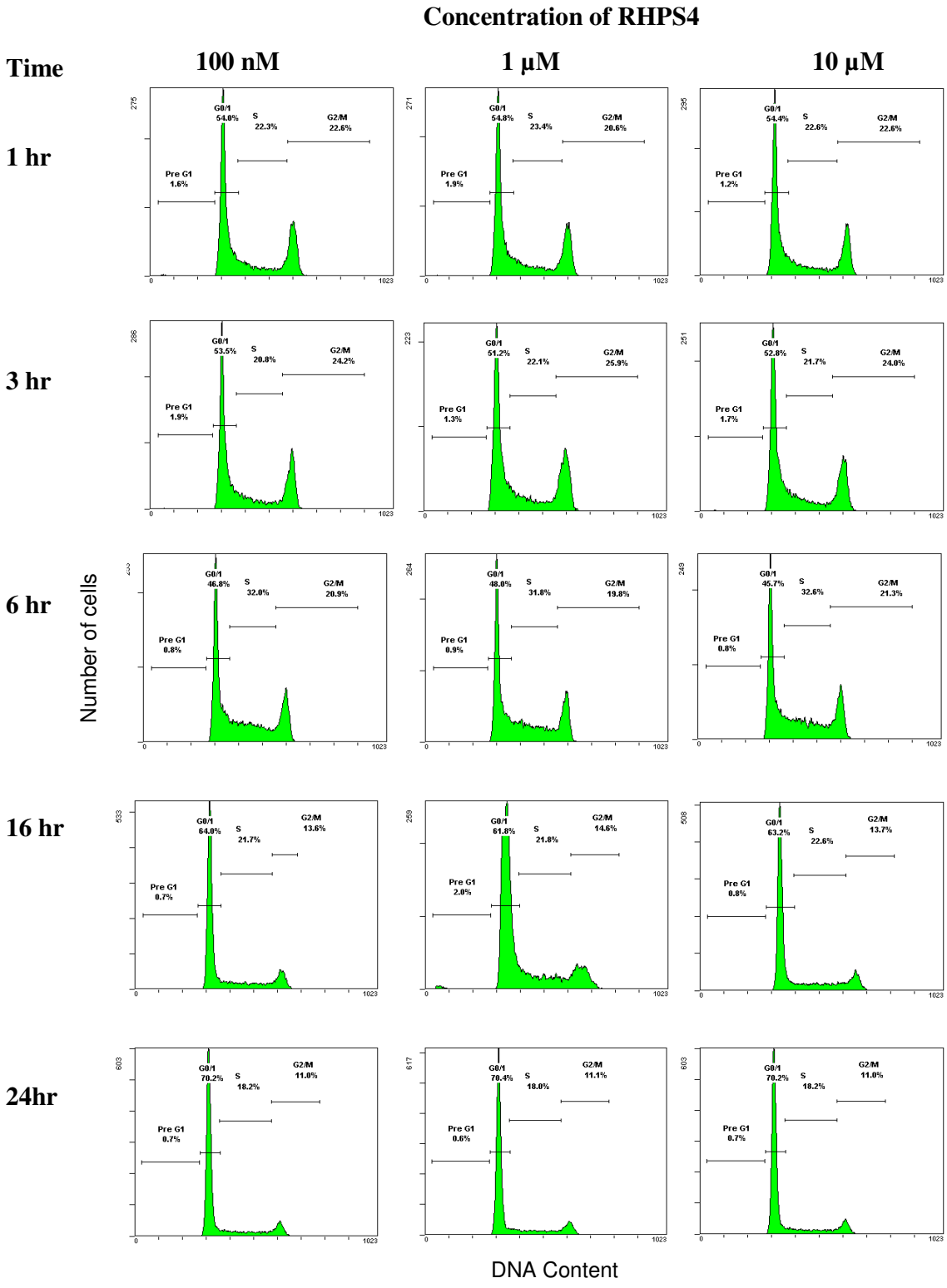


Figure 3.9 Cell cycle distributions of the short-term effects of RHPS4 on HT-29 cells up to 24 hours at 100 nM, 1 µM and 10 µM. The cells were collected as in chapter 2 using PI and analysed using flow cytometry measuring 20 000 events.

3.2.3.3 KM12

The KM12 cell line has very different growth characteristics from that of the other three cell lines analysed, however, appears to have a very similar short-term response to RHPS4. The cell cycle distribution of KM12 cells does not change significantly from that of the control up to 24 hours. Graphs of the change in cell cycle distribution in response to both time and concentration of RHPS4 are shown in figure 3.10 and typical DNA content histograms are shown in figure 3.11. These both demonstrate that there is no short-term effect of RHPS4 on the cell cycle of KM12 cells.

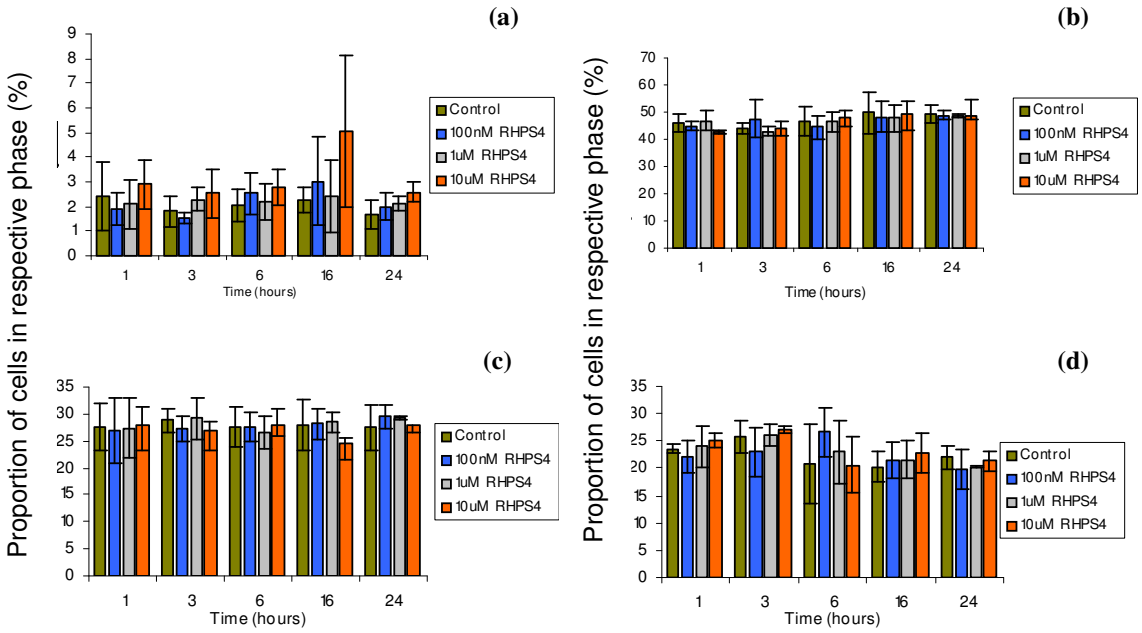


Figure 3.10 Short-term cell cycle distributions of KM12 cells in response to RHPS4. The cells were collected as in section 2.2.7.1 using PI and analysed using flow cytometry measuring 20 000 events and the proportion of cells in (a) pre-G_1, (b) G_1/G_0, (c) S and (d) G_2/M determined.

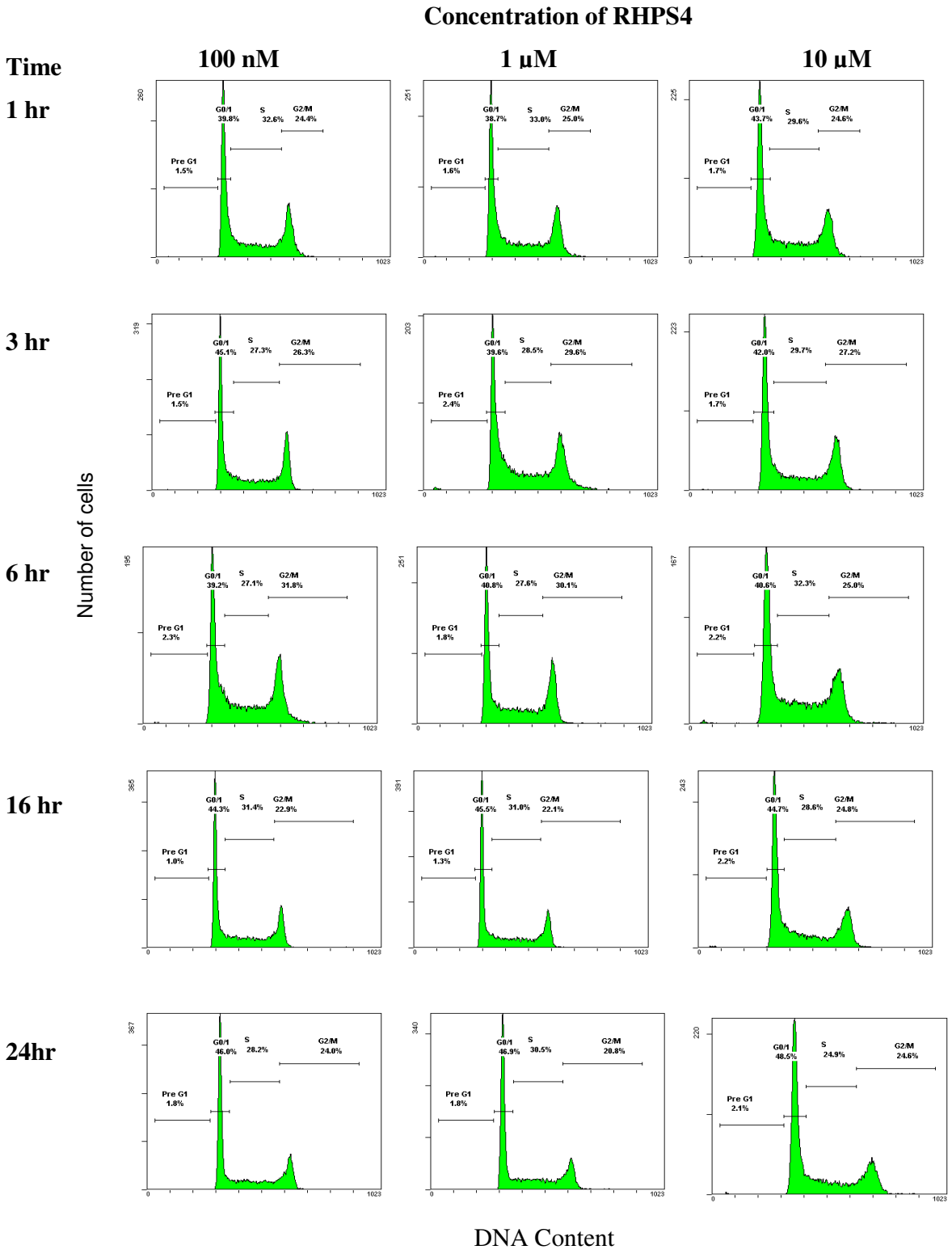


Figure 3.11 Cell cycle distributions of the short-term effects of RHPS4 on KM12 cells up to 24 hours at 100 nM, 1 µM and 10 µM. The cells were collected as in section 2.2.7.1 using PI and analysed using flow cytometry measuring 20 000 events.

3.2.3.4 HCC-2998

As with the other three cell lines analysed, there was no short-term effects of the cell cycle of HCC-2998 cells to RHPS4, however, they did show the least reproducible results. The largest variation was seen in the proportion of pre-G_1 and G_2/M cells as shown in figure 3.12, which shows graphical representations of the short-term response of HCC-2998 cells to RHPS4. Again, there were no significant differences between the cell cycle distributions of treated cell with that of control cells. Typical DNA histograms of HCC-2998 cells in response to RHPS4 are shown in figure 3.13.

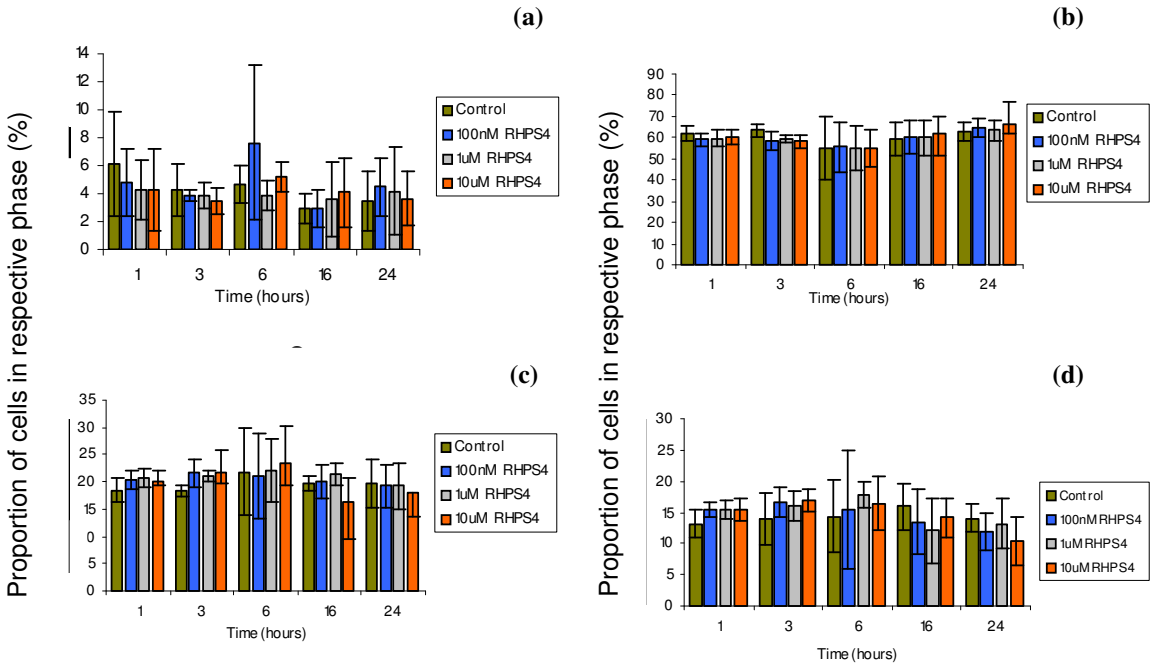


Figure 3.12 Short-term cell cycle distributions of HCC-2998 cells in response to RHPS4. The cells were collected as in section 2.2.7.1 using PI and analysed using flow cytometry measuring 20 000 events and the proportion of cells in (a) pre-G_1, (b) G_1/G_0, (c) S and (d) G_2/M determined.

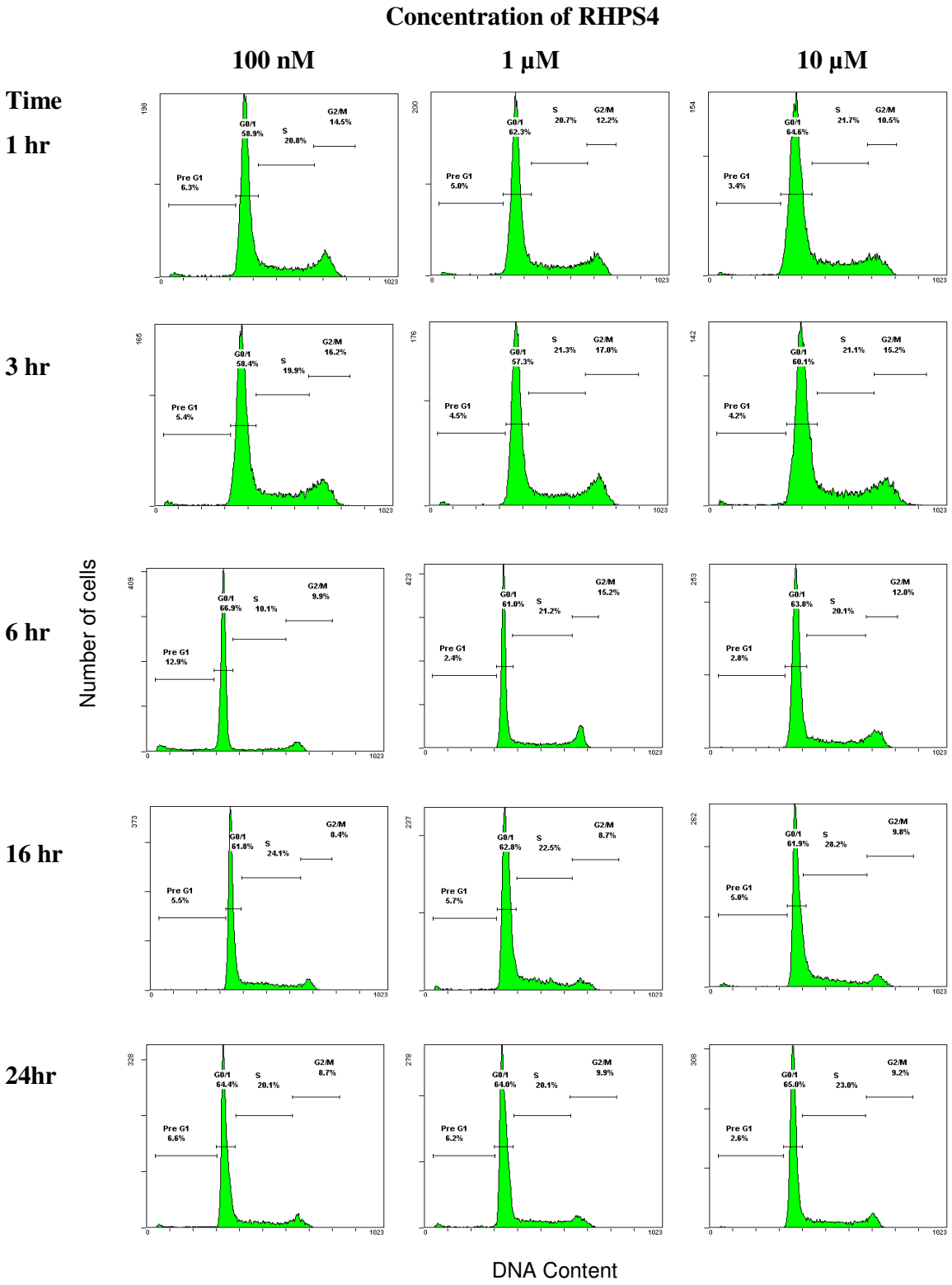


Figure 3.13 Cell cycle distributions of the short-term effects of RHPS4 on HCC-2998 cells up to 24 hours at 100 nM, 1 µM and 10 µM. The cells were collected as in chapter 2 using PI and analysed using flow cytometry measuring 20 000 events.

3.2.4 Long-Term Cell Cycle Responses to RHPS4

Following the analysis of the short-term effects of RHPS4 on the cell cycle of the four colorectal cell lines chosen for initial study, it was observed that there were no significant effects on the cell cycle distribution up to 24 hours with 100 nM, 1 μM and 10 μM RHPS4. The fact that there are no short-term effects of RHPS4 could be due to no initial effects on simple mechanisms within the cell that would cause short-term effects on the cells. The mechanism of action of RHPS4 may involve more complex actions within the cell that require longer times to manifest their effects. MTT assays, however, show that there is a reduction in cell viability when analysed up to 24 hours, and so shows that RHPS4 is having an effect with little perturbation of the cell cycle therefore the long-term effects of RHPS4 on the cell cycle were investigated. As with the short-term studies, HCT116, HT-29, KM12 and HCC-2998 cells were seeded and incubated with RHPS4 at concentrations of 100 nM, 1 μM and 10 μM. The cells were analysed following incubation periods of 24 hour, 48 hour, 72 hour, 96 hour and 120 hour and the results analysed via the flow cytometer.

3.2.4.1 HCT116

Under normal conditions, it appears that there is a basal level of pre-G_1 cells of 6%. The majority of cells appear to be in G_1/G_0 (62.13±3.22%) with approximately equal proportions in S and G_2/M (18.47±2.27% and 13.17±2.26%, respectively) and it appears that RHPS4 affects the cell cycle of HCT116 cells between 24-96 hours. At 24 hours, the proportion of cells in G_1/G_0 increases from the control, reaching a maximum of 66.20±5.07% at 48 hours in the presence of 1 μM RHPS4. At the same time, cells incubated in 10 μM RHPS4 have an increased proportion of cells pre-G_1 cells which increases further whereby at 72 hours the increase is significant in comparison to that of the control (two tailed p-value = 0.034). Cells incubated in 100 nM and 1 μM RHPS4 have a relatively stable proportion of cells in pre-G_1 throughout the duration of the experiment.

When analysing the effect of RHPS4 on the S phase of HCT116 cells, as before there is no evidence of any changes up to 24 hours and the proportion of cells in

this phase remains stable. At the higher concentration, however, the effects of 10 μM RHPS4 are apparent at 24 hours where the proportion of cells in S phase reduces from 27.93±2.28% at 6 hours to 7.57±3.55% by 24 hours. This decline continues to decline reaching a minimum at 48 hours whereby the proportion of cells decreases to 2.93±2.33% after which the proportion of cells in S phase increases again reaching 10.35±2.76% at 144 hours. The effects of 100 nM and 1 μM on the S phase of the cell cycle are also not apparent until 24 hours where they also show a reduction compared to the control, however do not reach the minimum that 10 μM achieves.

RHPS4 does not seem to effect the G_2/M phase of HCT116 cells, however at 48 hours and beyond, incubation with 10 μM RHPS4 induces an increase in the proportion of cells in G_2/M from 28.54±6.04% in control cells to 15.47±6.29% when treated, however this is non-significant (two-tailed p-value= 0.061). Cell cycle profiles are shown in figure 3.14 and show how the proportion of cells in each phase changes with respect to both time and concentration of RHPS4.

In addition, and in line with figure 3.7, RHPS4 also appears to cause S phase emptying in HCT116 cells when incubated with RHPS4 for up to 96 hours. Figure 3.14 shows this is a delayed effect and does not occur until 72 hours, however, remains until 96 hours, where at concentrations of 100 nM and 1 μM, there appears to be a delayed effect. At these concentrations, there appears to be a delayed effect and the cells are overcoming the S phase clearance, which does not appear evident at the higher concentration of 10 μM. What is evident, however, at the higher concentration of RHPS4 is the shift of the histogram to the right which is suggestive of a change in the access of the fluorophore, PI, to the DNA. Figures 3.15 - 3.17, which depict the effect of RHPS4 on HT-29, KM12 and HCC-2998 cells up to 96 hours, respectively, do not appear to have this S phase clearance and may be due to differences in p53 status. HCT116 cells, as shown in table 3.1, are the only cell line of the four chosen that has wild-type p53 status. Due to their status, HCT116 cells display a normal p53 response. p53 can be activated in response to cellular stress or DNA damage and has a number of effects including suppression of cell growth, cell cycle arrest or apoptosis (Joseph *et al*, 2005). The

S phase clearance displayed in HCT116 cells, and not KM12, HT-29 or HCC-2998 cells could be the result wild-type p53 status versus mutant p53 status.

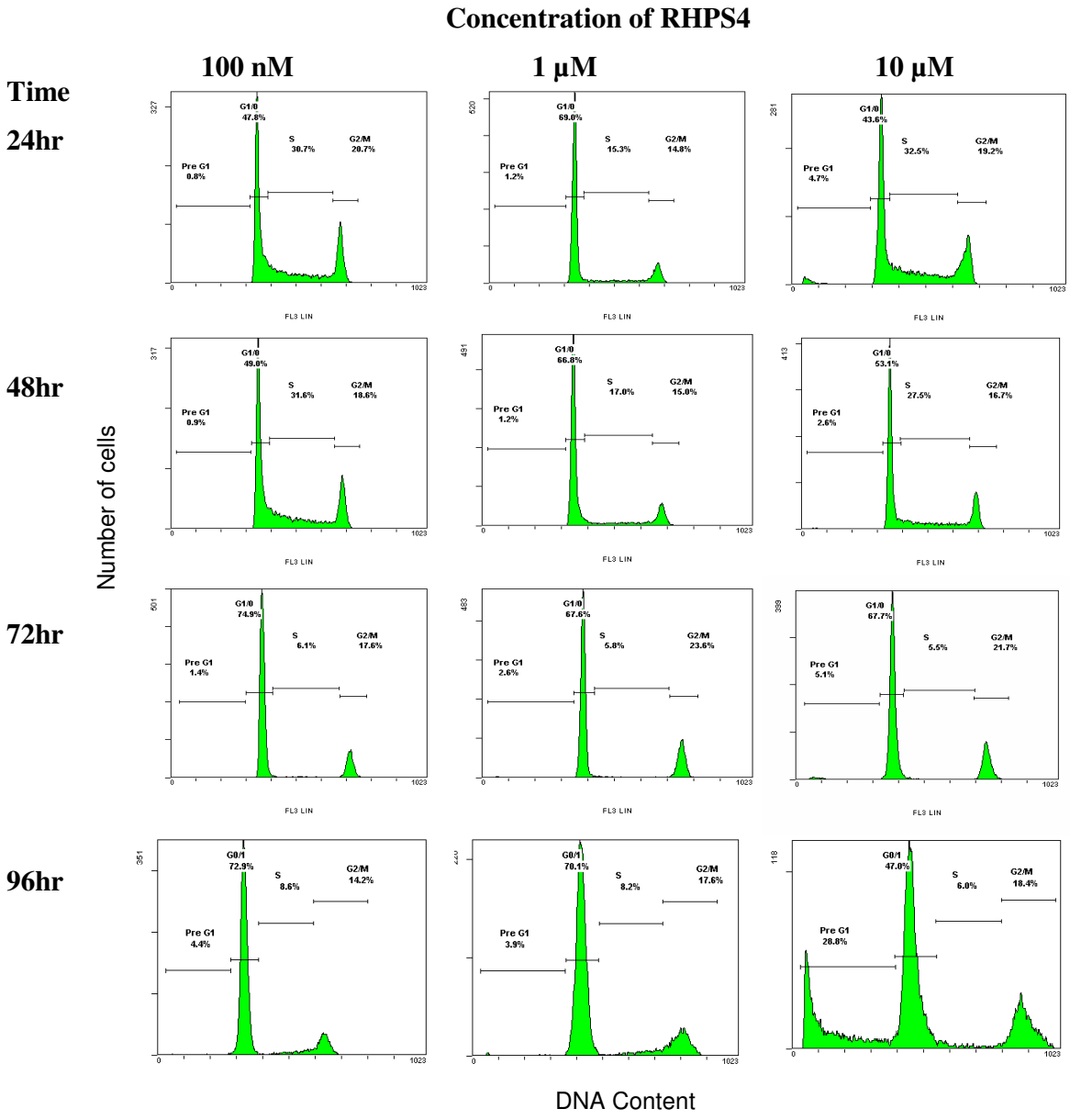


Figure 3.14 Long-term effects of RHPS4 on the cell cycle of HCT116 cells up to 96 hours. Typical cell cycle distributions following incubation with RHPS4 at concentrations of 100 nM, 1 µM and 10 µM up to 96 hours and analysed on the flow cytometer measuring 20 000 events.

3.2.4.2 HT-29

The effects of RHPS4 on the cell cycle of HT-29 cells are similar to those for HCT116 cells. Under normal conditions, HT-29 cells have a distribution of pre-G_1: 1.82±0.74%, G_1/G_0: 49.18±4.90%, S: 22.19±4.70% and G_2/M: 11.02±3.10%. The presence of 10 μM RHPS4 has no significant effect on pre-G_1 between 1-72 hours. However at 96 hours, the percentage of pre-G_1 cells increases significantly in comparison to control (two-tailed p-value = 0.031). In the presence of either 100 nM or 1 μM RHPS4, the proportion of pre-G_1 cells does not vary from that of the control cells.

Analysing the effect of RHPS4 on G_1/G_0 phase of HT-29 cell, again there is no significant variation from the control. At 24 hours, the proportion of cells in G_1/G_0 increases from 60% to 66% and remains relatively stable until 144 hours for all conditions. A maximum of 71.25±4.74% is achieved by the presence of 1 μM RHPS4 at 96 hours, however in comparison to control, is non-significant (two-tailed p-value = 0.535).

When analysing the effects of RHPS4 on S phase, there appears to be no effect in comparison to control with the averages of 100 nM RHPS4: 24.66±8.16%, 1 μM RHPS4: 22.46±4.41%, 10 μM RHPS4: 21.78±4.97%. A maximum of 48% of cells in S phase is achieved by 100 nM at 72 hours, but again this is non-significant in comparison to control (two-tailed p-value= 0.268). RHPS4 also has no significant effect on the G_2/M phase of HT-29 cells. At 24 hours, the effect of RHPS4 is concentration-dependent with the maximum achieved by 10 μM RHPS4 however the increase from the control is non-significant (two-tailed p-value = 0.755). Overall there appears to be no significant effects on the cell cycle of HT-29 cells.

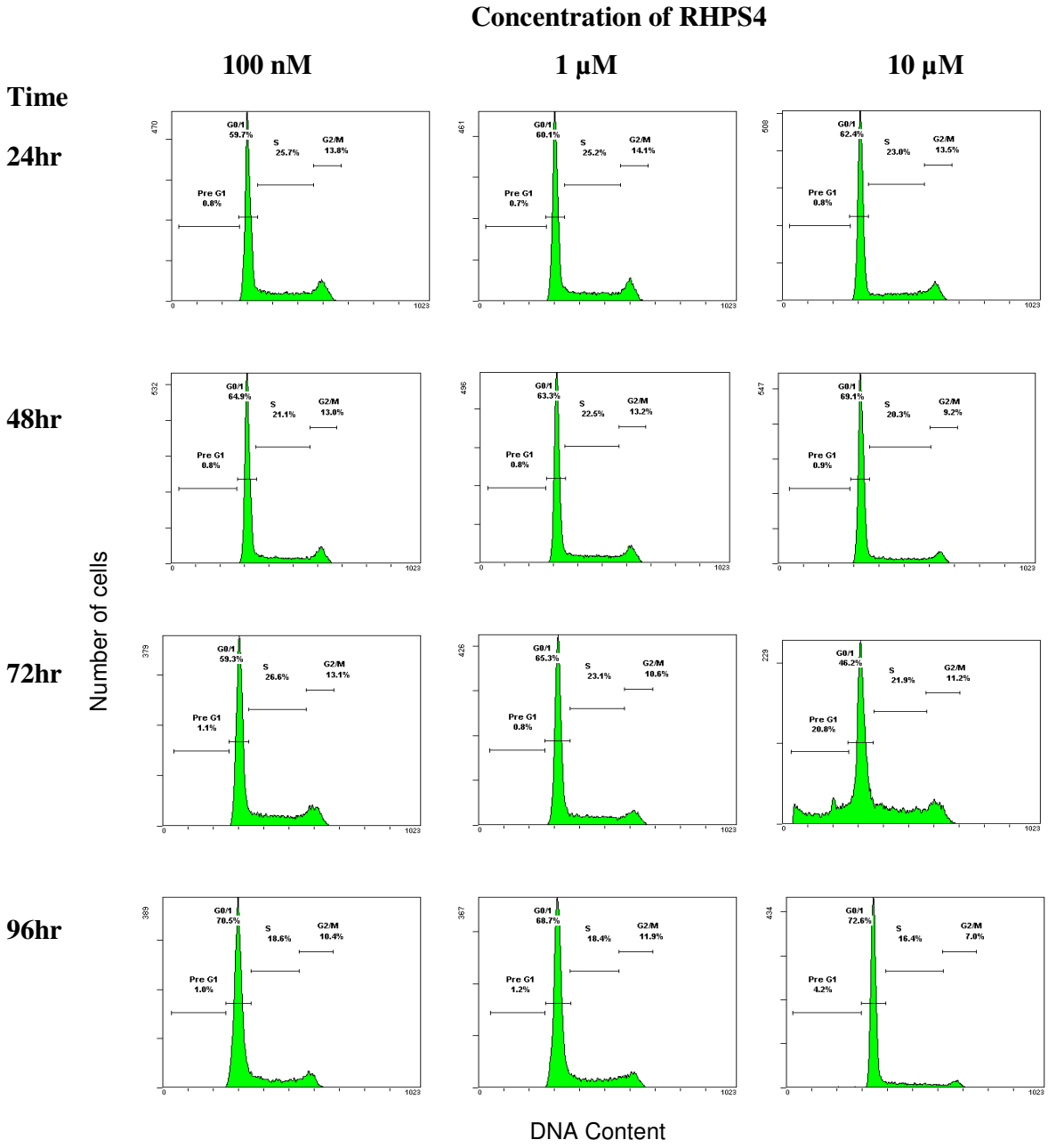


Figure 3.15 Long-term effects of RHPS4 on the cell cycle of HT-29 cells up to 96 hours. Typical cell cycle distributions following incubation with RHPS4 at concentrations of 100 nM, 1 µM and 10 µM up to 96 hours and analysed on the flow cytometer measuring 20 000 events.

3.2.4.3 KM12

Under normal conditions, the cell cycle profile of KM12 cells appears to be pre-G_1: 3.25±1.84%, G_1/G_0: 44.69±3.74%, S: 32.79±2.64% and G_2/M: 23.49±2.56%.

Upon treatment with RHPS4 there are no noticeable changes with either concentration or time up to 48 hours on the cell cycle profile. Between 48-144 hours, the presence of 10 μM RHPS4 increases the proportion of pre-G_1 cells in comparison to the lower concentrations of RHPS4 and the control. At both 96 and 144 hours, the increase in pre-G_1 cells is significant in comparison to the control with two-tailed p-values of 0.034 and 0.013, respectively. There are no effects of RHPS4 on G_1/G_0, even at the highest concentration until 48 hours, after which 10 μM RHPS4 reduces the proportion of cells in this phase. In both 1 μM and 100 nM RHPS4 there is an increase in comparison to the control of cells in G_1/G_0, reaching a maximum of 51.27% in the presence of 100 nM RHPS4 at 72 hours.

Analysing the effect of RHPS4 on the S phase of the cell cycle of KM12 cells, there are again no significant changes between up to 48 hours. By 72 hours, the presence of RHPS4 at 100 nM and 1 μM reduces the proportion of cells in S phase in comparison to the control. Analysis of the effect of RHPS4 on the G_2/M phase of the cell cycle again shows no noticeable changes up to 48 hours, after which there is a concentration -dependent effect occurring. The presence of 1 μM RHPS4 increases the proportion of cells in G_2/M in comparison to the control whilst incubation with 10 μM or 100 nM RHPS4 actually reduces the proportion of cells in the G_2/M phase of the cell cycle.

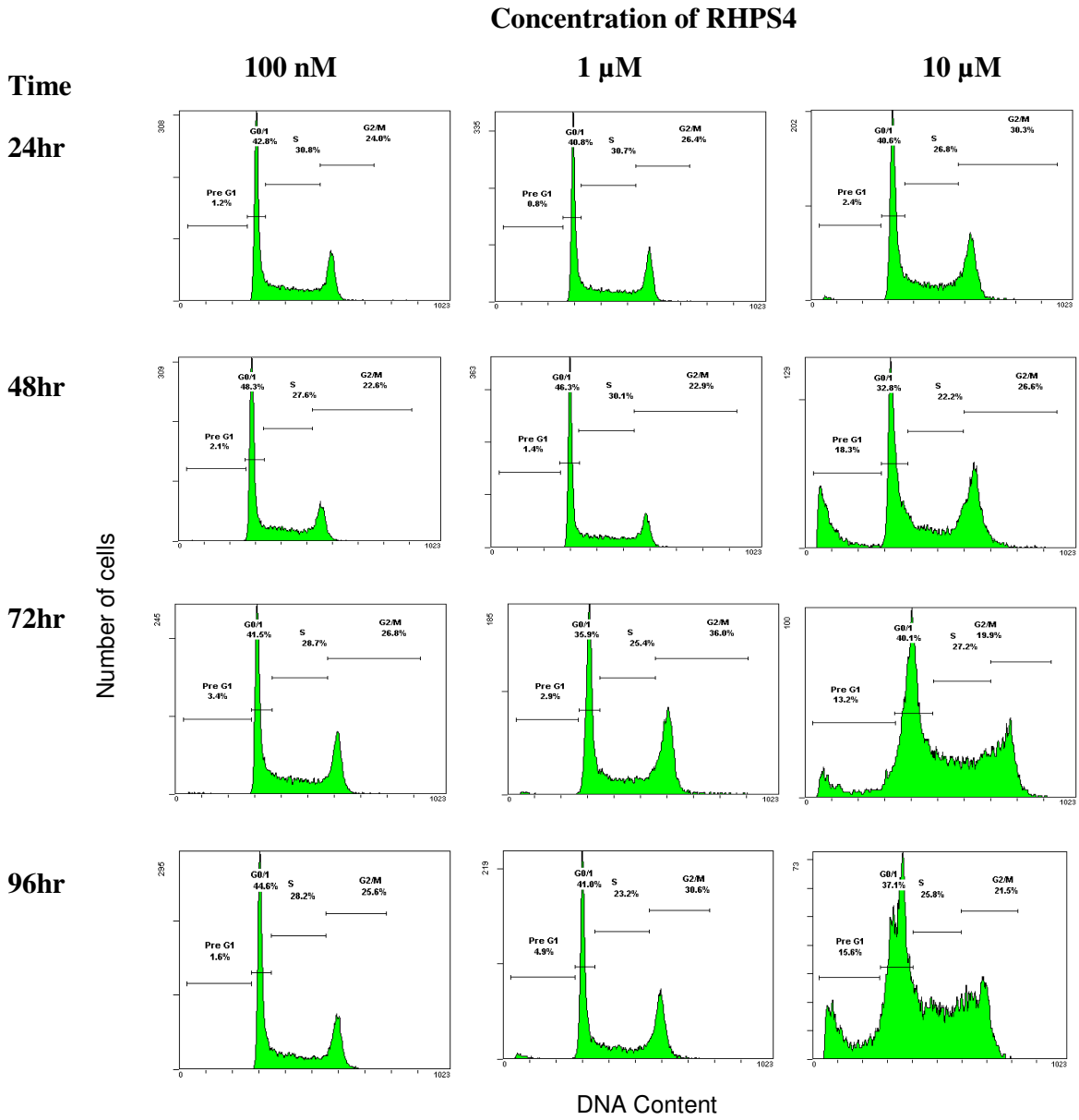


Figure 3.16 Long-term effects of RHPS4 on the cell cycle of KM12 cells up to 96 hours. Typical cell cycle distributions following incubation with RHPS4 at concentrations of 100 nM, 1 µM and 10 µM up to 96 hours and analysed on the flow cytometer measuring 20 000 events.

3.2.4.4 HCC-2998

As with the MTT assay results, the HCC-2998 cell line produced quite variable and unpredictable results. When analysing the effect of RHPS4 on the cell cycle, the results were often irreproducible, however, typical DNA content histograms of HCC-2998 cells in response to RHPS4 are shown in figure 3.17. The typical cell cycle profile of HCC-2998 cells under normal conditions appears to be: pre-G_1:

5.10±1.28%, G_1/G_0: 60.28±2.94%, S: 21.34±2.51% and G_2/M: 13.22±1.52%. Upon treatment with 10 μM RHPS4, there is an increase in the proportion of cells in G_1/G_0 and pre-G_1. The increase in the proportion of cells in pre-G_1 was consistent; however, the increase in the proportion of cells in G_1/G_0 was variable and unpredictable, suggesting therefore that 10 μM is quite toxic to HCC-2998 cells and causes cell death and are consistent with the MTT assay results. At the lower concentrations, there appeared to be no effect of RHPS4 up to 24 hours, however, incubation with either 100 nM or 1 μM RHPS4, appears to increase the proportion of cells in G_1/G_0, whilst reducing the proportion of cells in S and G_2/M. The effect is greater in cells incubated with 1 μM RHPS4.

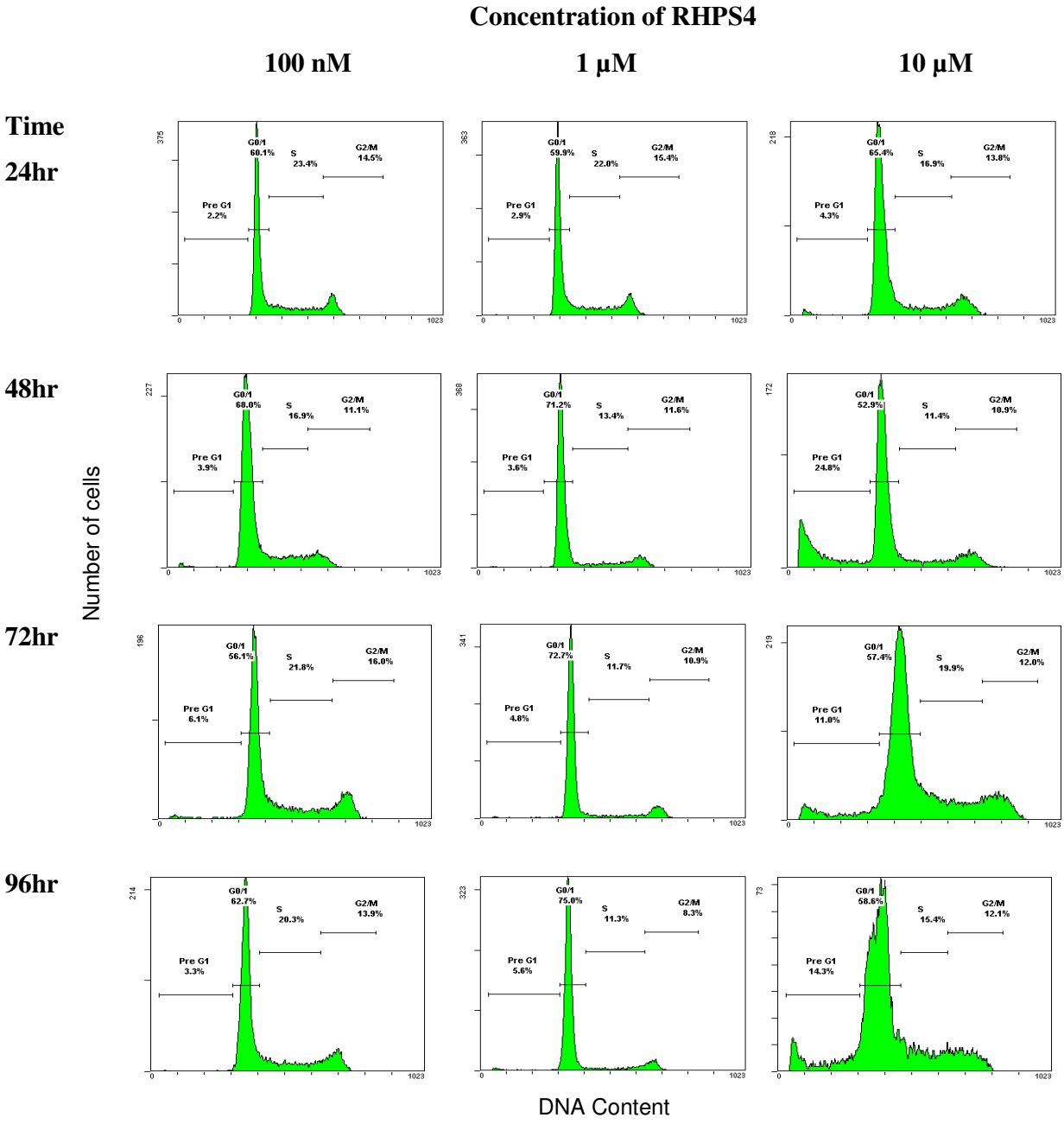


Figure 3.17 Long-term effects of RHPS4 on the cell cycle of HCC-2998 cells up to 96 hours. Typical cell cycle distributions following incubation with RHPS4 at concentrations of 100 nM, 1 µM and 10 µM up to 96 hours and analysed on the flow cytometer measuring 20 000 events.

3.2.5 Analysis of the Effects of RHPS4 on Population Doublings

So far the effect of RHPS4 on cell viability and both the short-term and long-term effects on colorectal cell lines have been analysed. The purpose is the selection of an appropriate cell line which is robust with well-defined characteristics and

reproducible results for further analysis and the development of a mathematical model. The aim of a mathematical model is to derive information regarding the effects of RHPS4 on colorectal cell lines that would otherwise be difficult to appreciate without it. To further investigate the robustness and reliability of the four colorectal cell lines chosen for initial study, the number of doublings of each cell line over a 21 day period was analysed with the aim to find which of the cell lines complete the greatest number of population doublings. Due to the slow growth and unreliability of the results of HCC-2998, it was decided that they would not be an appropriate cell line for the development of a mathematical model. It was therefore decided that no further analysis of the effects of RHPS4 on HCC-2998 cells would take place.

A graphical representation of the number of doublings completed by HCT116, HT-29 and KM12 are shown in figure 3.18. From this graphs, it is evident that over a 21 day period, HCT116 cell complete an average 14.63 doublings, whilst KM12 complete only an average 8.55 doublings. HT-29 cell complete an average 11.79 doublings. The data shown in figure 3.18 is inconsistent with the data regarding doublings times, shown in table 3.1 and is likely to be an artefact of the experimental design. Short-term cell cycle studies do not require interference, whereas longer term studies up to 21 days required the counting of the cells at days 4, 6, 10, 14 and 21. Upon counting the cells, they are re-subbed at the required density and they will require time to establish and therefore affecting the number of doublings throughout the experiment.

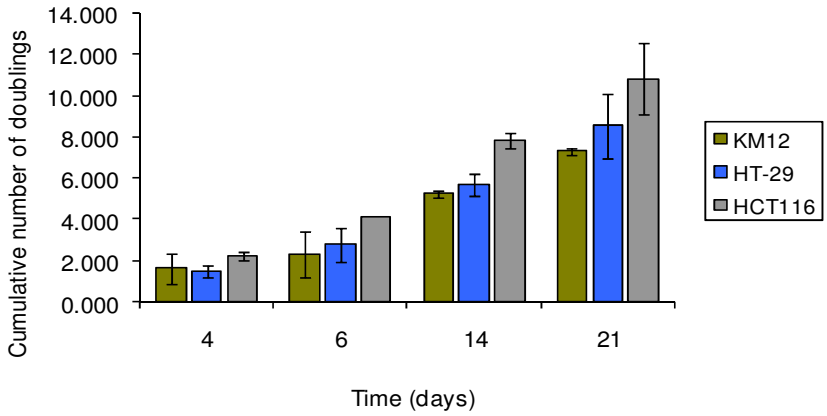


Figure 3.18 Population doublings of KM12, HT-29 and HCT116 cells over 21 days. The population doublings of KM12, HT-29 and HCT116 cells were analysed under normal conditions over 21 days and were analysed using a haemocytometer.

3.2.6 Analysis of the Effects of RHPS4 on Senescence

Normal cells have limited proliferative potential in culture, a fact that has been the basis of their use as a model for replicative senescence for many years. Recent molecular analyses have identified numerous changes in gene expression that occur as cells become senescent, and the results indicate that multiple levels of control contribute to the irreversible growth arrest (Smith & Pereira-Smith, 1996). To investigate the ease of senescence analysis of HCT116, HT-29 and KM12 cells, they were incubated with GI_{25}, GI_{50} and GI_{75} concentrations up to 21 days. The concentrations used are shown in table 3.3. The aim of this investigation was to find which of the three cell lines, HT-29, HCT116 or KM12 had the 'best' morphology to assist in analysing senescence and increase the number of parameters to be included in the mathematical model.

Table 3.3: Concentration range of RHPS4 used to analyse the effects on senescence of HCT116, HT-29 and KM12 cells

Cell Line	GI_{25} concentration	GI_{50} concentration	GI_{75} concentration
HCT116	50 nM	100 nM	1 μM
HT-29	50 nM	0.5 μM	1 μM
KM12	2 nM	5 nM	10 nM

3.2.6.1 HCT116

The HCT116 cell line appeared to have the best morphology to facilitate in the analysis of senescence in response to RHPS4. When analysing senescence, the cells were stained with β-galactosidase at pH 6 (Dimri *et al*, 1995). Following incubation of the cells with the stain, five random images were taken and each image analysed and an average proportion of stained cells from the five images calculated. Typical images of HCT116 cells in response to RHPS4 with respect to time and concentration are shown in figure 3.19. It is evident that under normal conditions, there is a basal level of senescence of approximately 10%. It was also evident that there was a concentration- and time- dependent increase in the proportion of senescent cells. This is evident from the images shown in figure 3.19, which show that at the highest concentration of 1 μM there is an increase in the proportion of senescent cells, which increases to reach a maximum at day 21. This pattern is also evident in cells incubated with either 50 nM or 100 nM RHPS4.

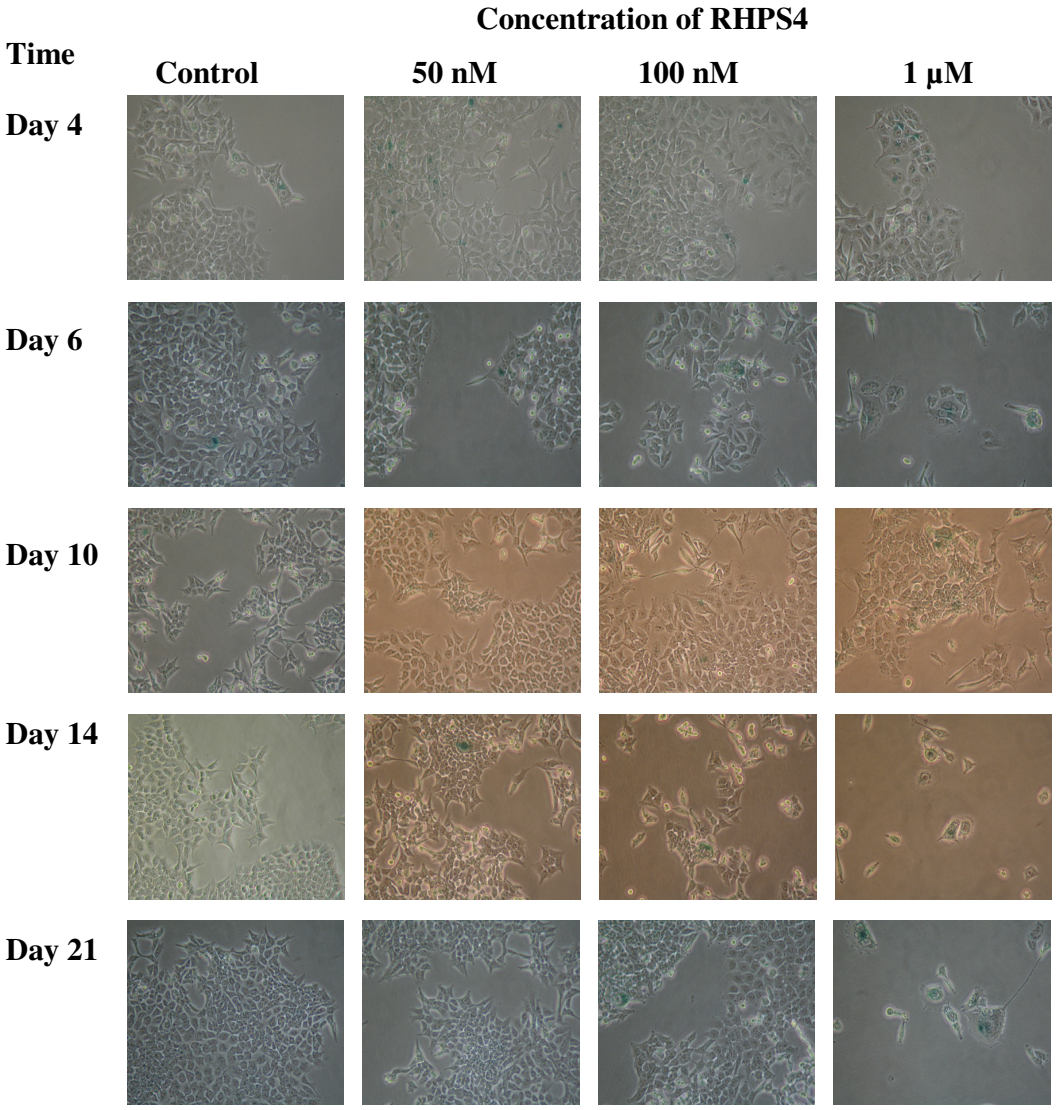


Figure 3.19 Senescence images of HCT116 cells in response to RHPS4. The cells were incubated with a range of concentrations of RHPS4 and senescence levels analysed using the SA-β-gal method at days 4, 6, 10, 14 and 21. Digital images of 5 random fields of view were analysed and shown here are typical images derived.

3.2.6.2 HT-29

The HT-29 cell line displayed a high level of senescence in response to RHPS4 and under normal conditions. The HT-29 cell line was exposed to 50 nM, 0.5 µM and 1 µM RHPS4 and it was discovered that exposure to concentrations of 0.5 µM or 1 µM were too toxic at these time points for the cells as can be seen in figure 3.20. It is possible that at these concentrations they would be false positives as the cells are possibly senescent due to other factors, such as lack of surrounding

cells so the cells have entered quiescence and the positive stain is not senescence in response to the presence of RHPS4. The earlier determination of these concentrations of RHPS4 on HT-29 cells did not highlight the toxicity simply because of the length of the experiments. The earlier experiments were carried out up to 144 hours and no toxicity was detected and as figure 3.20 shows, there is no toxicity detected at day 4, however, there is senescence detected. The senescence experiments were carried out up to 21 days and it appears that at the higher concentrations of 0.5 μM and 1 μM, there is a level of toxicity observed.

The basal level of senescence in cells under normal conditions remained throughout the 21 day period. Unlike HCT116 cells, the morphology of HT-29 cells makes it quite difficult to quantitatively analyse the proportion of senescent cells within a population. For a mathematical model, we would require as many components of the cell cycle to be incorporated as possible and the lack of senescence data from the HT-29 cell line will inevitably reduce the accuracy of the mathematical model and any possible conclusions which can be drawn from that.

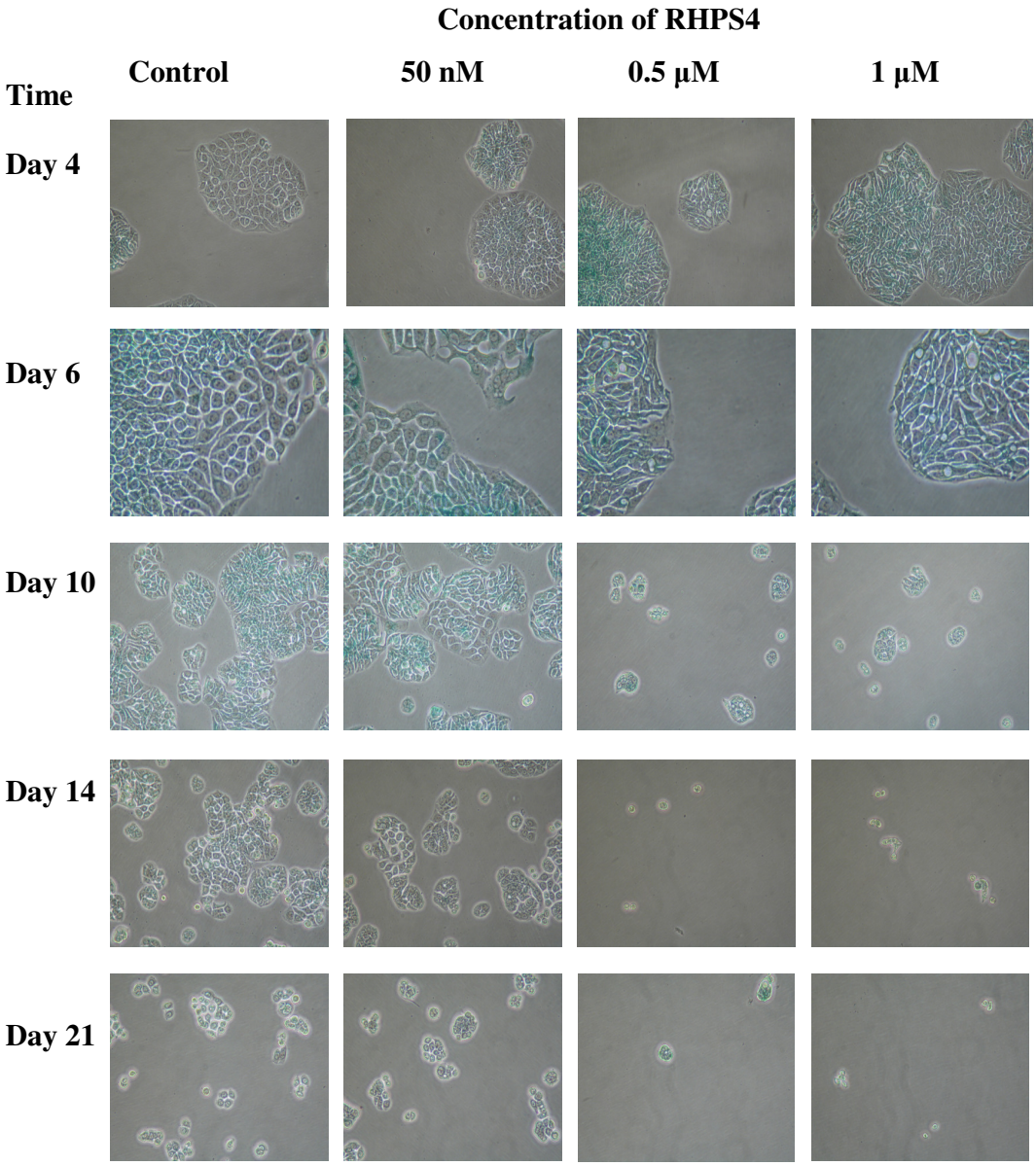


Figure 3.20 Senescence images of HT-29 cells in response to RHPS4. The cells were incubated with a range of concentrations of RHPS4 and senescence levels analysed using the SA-β-gal method at days 4, 6, 10, 14 and 21. Digital images of 5 random fields of view were analysed and shown here are typical images derived.

3.2.6.3 KM12

Senescence analysis of KM12 cells was very difficult due to their growth morphology as can be seen in figure 3.21. The cells were incubated for up to 21 days in 2 nM, 5 nM and 10 nM RHPS4. At all time points and agent concentrations, KM12 cells are observed in 'clumps' making cell counting difficult and so it was decided that this cell line would not be used for the

development of a mathematical model to investigate the mechanism of action of RHPS4.

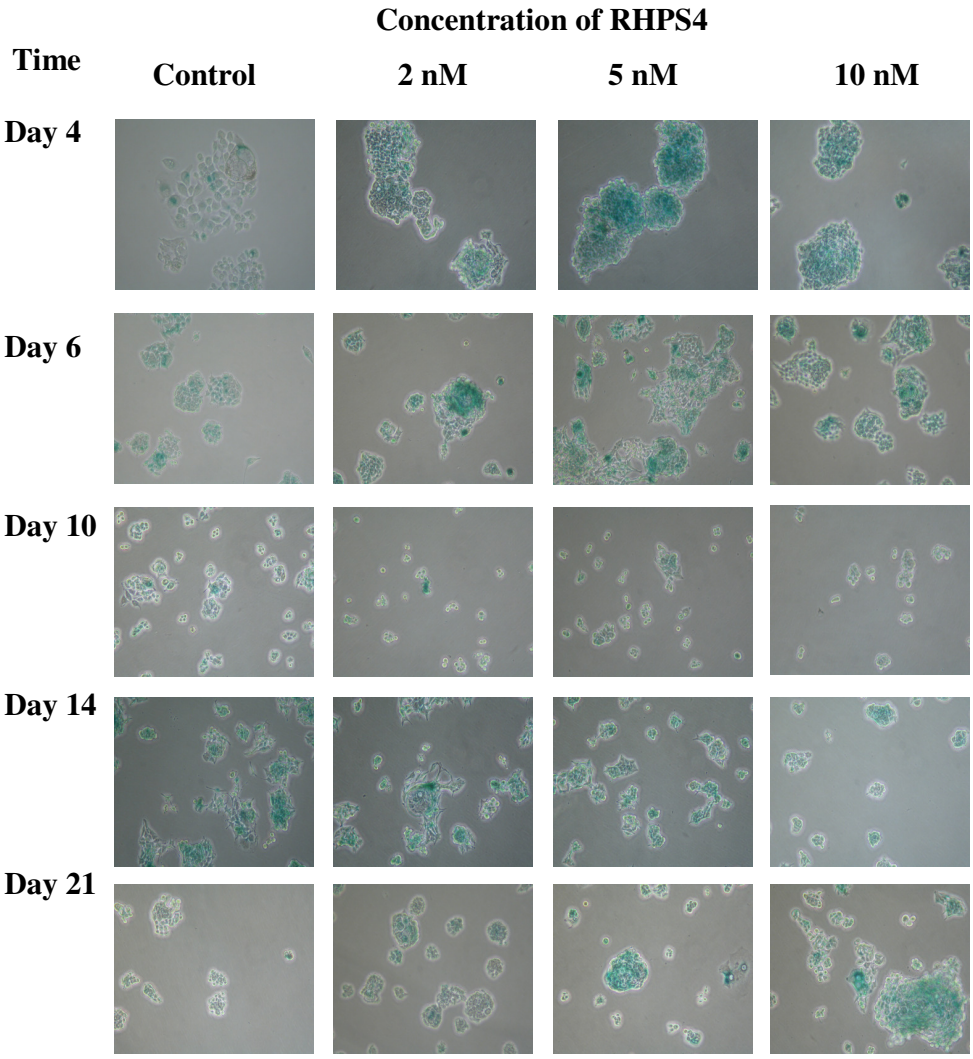


Figure 3.21 Senescence images of KM12 cells in response to RHPS4. The cells were incubated with a range of concentrations of RHPS4 and senescence levels analysed using the SA-β-gal method at days 4, 6, 10, 14 and 21. Digital images of 5 random fields of view were analysed and shown here are typical images derived.

3.3 Estimating the Pre-G_1 Fraction

The point of this analysis is to determine the reasons for these differences and explore the ways in which pre-G_1 can be calculated. As stated previously, the method used for cell cycle analysis in this thesis is the Nicoletti method and

although this does identify a pre-G_1 fraction, this fraction is representative of cell degradation products and 'dead' cells. Due to this, a more appropriate analysis of cell apoptosis versus cell death is required to validate exactly what the pre-G_1 fraction is representative of. It is known that the pre-G_1 fraction could include mechanically damaged cells, cells with reduced chromosome number, apoptotic bodies and nuclear fragments from a single apoptotic cell. The most sensible approach is the removal of debris and cell degradation products using the gating structures as outline in appendices I and II. Appendix I describes how the data is extracted, whilst appendix II described how the data is analysed. From the gating out of the cell degradation products and cell debris, it is appropriate then to analyse the G_1/G_0, S and G_2/M fractions. The cell death fraction can then be analysed separately as shown in this section. As outlined in appendix II, the current histograms presented in section 3.2.3 and 3.2.4, were analysed using the manual method which is appropriate since the data is short term in nature. The present study aims to use a systems biology approach to the analysis of RHPS4 and the conclusion drawn in appendix II is that the current method of analyzing the pre-G_1 fraction is inappropriate since it is over-estimated and the viable fraction is under-estimated. In addition, the non-cycling fraction is under-estimated since on the cell cycle histogram the G_1 peak is representative of both G_1 and G_0 and we cannot distinguish them using PI, hence the attempts in section 3.4 to differentiate between G_1 and G_0. In this section is an analysis of the different methods available for the accurate analysis of cell death.

The easiest method of analysing the cell death fraction is the manual method and taking pre-G_1 to be equal to cell death since this can be derived using Expo32™ software, however, is inaccurate since it is thought this method provides an over-estimate. The reason for this over-estimate is due to the fact that the pre-G_1 fraction, as stated previously, incorporates not only apoptotic cells, but also cell fragments and cellular debris so this method assumes that one event is the equivalent of one cell and this is not the case. This method was used to analyse the histograms in sections 3.2.3 and 3.2.4. To compare and contrast with this, is another method whereby the data is segmented using the appropriate dot plots as

outlined in section 2.2.7.2, and the cell death fraction is calculated based on fluorescence intensity as shown in equation 3.1 below.

$$n_d = \frac{\Sigma n_i I_i}{I_{g_1}} \quad \textbf{(3.1)}$$

Where n_d is the total number of dead cell

n_i is the number of cell fragments with intensity I_i

I_i is the intensity of a pre-G_1 cell fragment

I_{g1} is the intensity of a G_1 cell

In order to determine the intensity of a cell or cell fragments, the software package, Cylchred or winMDI are available. Cylchred is an automated cell cycle analysis software package available from Cardiff University and accepts histograms in the FCS single binary format. Cell cycle analysis is performed based on the gaussian fit as Cylchred adds at least two gaussians to the histogram and from this is able to calculate the proportion of cells in G_1/G_0, S and G_2/M. Based on the intensity of cells in the G_1/G_0 fragment, we can use equation 3.1 to determine the proportion of cells in the pre-G_1 fragment. Cylchred invokes the main cell cycle algorithm and displays the derived components on the histogram with the associated data in the results window. Within the fitted region, the residual G_1, G_2 and S phase components are calculated. WinMDI is a software package that can be used to gate a multiparameter LMD file and produce a 'clean' DNA histogram in the active window that can then be saved as a FCS binary file that can then be viewed in Cylchred and the proportion of cells in each phase calculated.

Table 3.4: Comparison of the data derived from the original method used and that using equation 3.1

Cell cycle phase		**Pre-G_1**	**G_1/G_0**	**S**	**G_2/M**	**Pre-G_1**	**G_1/G_0**	**S**	**G_2/M**
Condition	**Time (hours)**	**Original Data**				**New Data**			
Control	**24**	1	44.6	30.8	24	0.09	31.44	50.96	17.6
100 nM RHPS4	**24**	1.2	48.5	30.7	20.5	0.58	33.92	50.98	15.1
1 µM RHPS4	**24**	0.8	47.1	30.1	22.8	0.29	35.33	50.46	35.33
10 µM RHPS4	**24**	2.2	43.2	27	27.7	0.61	36.84	55.79	7.88
Control	**48**	1.5	44.1	22	33.4	0.72	34.26	53.09	12.65
100 nM RHPS4	**48**	2	51	30.4	17.1	0.82	39.02	48.84	12.15
1 µM RHPS4	**48**	1.4	49.5	28.7	21	0.64	36.55	45.05	18.40
10 µM RHPS4	**48**	19.1	34.9	18.2	28.1	4.92	22.53	53.79	23.69
Control	**72**	3.1	40.2	16.8	31.5	0.24	39.14	47.62	13.24
100 nM RHPS4	**72**	1.5	47	30.4	21.4	1.38	33.74	53.56	12.7
1 µM RHPS4	**72**	2.9	38.1	28.5	30.6	0.95	36.83	48.38	14.79
10 µM RHPS4	**72**	11.5	40.5	31.5	16.8	5.68	36.83	48.38	14.79
Control	**96**	1.8	46.2	24	28.3	0.08	30.01	53.25	16.73
100 nM RHPS4	**96**	1.6	44.6	28.3	26.2	0.51	32.36	51.18	16.46
1 µM RHPS4	**96**	4.9	41.6	23.2	31	1.26	37.15	49.28	13.57
10 µM RHPS4	**96**	15.8	42.2	26.6	15.7	3.12	40.04	46.02	13.94

Table 3.4 depicts the same dataset from the KM12 cell line via the Nicoletti method as described in section 2.2.7 and via equation 3.1 to allow for their comparison and determine which is considered to be the best way of analysing the long term data, which will ultimately be applied to the mathematical model. Since we have no 'genuine' numbers, we cannot really say which is the most accurate and instead can determine how different they are and how the overall conclusions are affected. It is evident from table 3.3 that the proportion of cells in S phase are larger when using Cylchred and may be due to the way in which the Gaussian fit appears to work. Cylchred works by fitting a Gaussian function to the

histogram, however, the manual method works by applying markers. In applying markers, there is subjectivity and could lead to incorporation of small percentages of the S phase into the proportion of cells in G_1/G_0 and G_2/M.

The original method appears to over-estimate the pre-G_1 fraction; however, the concentration-dependent increase in pre-G_1 is still present. For example, at a concentration of 10 μM at 24 hours, the original method calculated 2.2% cell death, whereas the new method estimated there to be 0.61%. Increasing the period of incubation to 48 hours increases the proportion of cell death to 19.7% according to the original method and to 4.92% according to the new method of analysis. The corresponding control at 24 hours shows there to be 1% cell death in accordance with the original method and 0.09% according to the new method. At 48 hours, there appears to be 1.5% cell death according to the original method and 0.72% according to the new method. The examples are the raw data from one set of experiments and therefore there is no average or standard deviation calculated.

Another method that would be acceptable for the analysis of the pre-G_1 fraction would be the analysis of the viable fraction against the non-viable fraction. The viable fraction would incorporate the cycling cells, i.e. G_1/G_0, S and G_2/M, whilst the non-viable fraction would include cells that were part of the pre-G_1 fraction and would be calculated using the software packages Cylchred and WinMDI. In doing this, the viable fraction would be much less noisy and the confidence in the estimation of the viable cells would be increased since there would be no influence of non-viable of pre-G_1 cells. Figure 3.22 depicts the original data from KM12 cells incubated for up to 96 hours with RHPS4 at concentrations of RHPS4 between 100 nM and 10 μM. Figure 3.23, however, depicts the data from table 3.4. Both sets of data for figures 3.22 – 3.23 were analysed in the same way to highlight the differences in the methods chosen to analyse the cell cycle and how this can impact on the final results. It is important to note that the aim is to identify the differences between the different methods of analysis and not identify which is the most accurate since we have no 'genuine' numbers. In addition, the aim of this section is to highlight the importance of data analysis and the need for high-quality data when taking a systems biology approach. To practice systems

biology, biological data from as many hierarchical levels of information as possible must be captured and integrated. This data needs to be vigorously analysed and be of a high-quality. This section highlights the importance of considering the different methods of analysis available and the impact this has on the approach being used and the final conclusions. It is clear from figures 3.22 – 3.23 that the viable versus non-viable method of analysis is not the best way forward since the mathematical model requires the specific proportions of cells in each phase of the cell cycle. To use the viable versus non-viable, although fine, would only allow us to determine the proportion of cells in G_1/G_0, S and G_2/M as a whole.

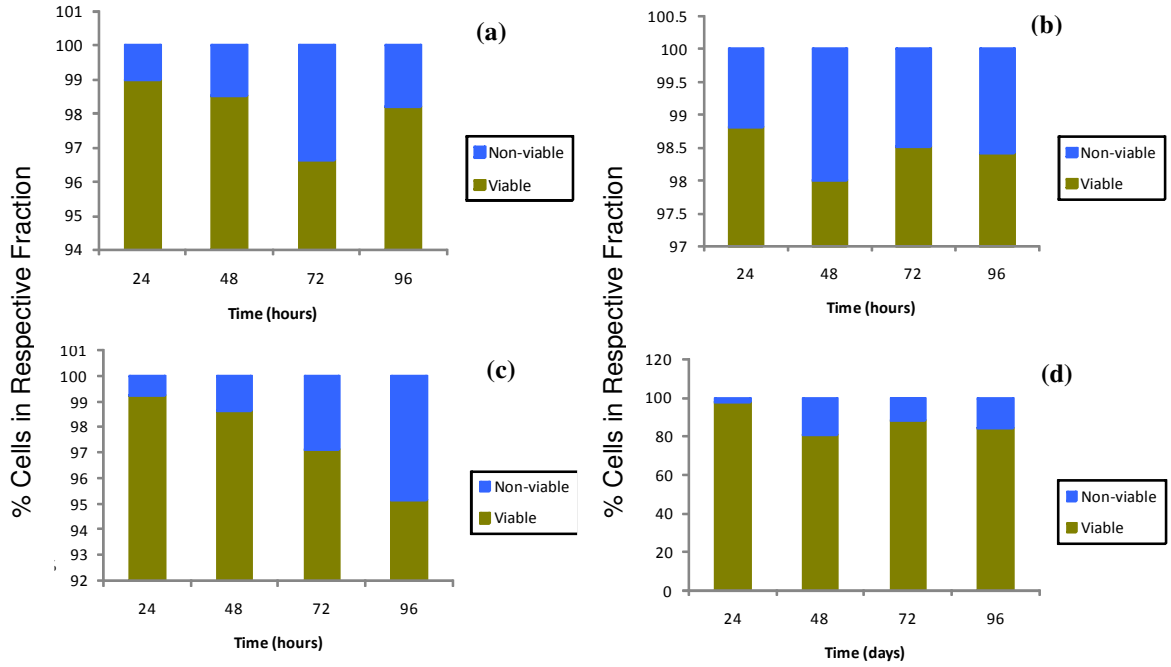


Figure 3.22 Analysis of the original data using the non-viable fraction against the viable fraction estimation. The viable fraction incorporates the cycling cells, i.e. those in G_1/G_0, S and G_2/M, whilst the non-viable fraction incorporates the pre-G_1 fraction. The results shown here depict the effects of (a) control, (b) 100 nM RHPS4, (c) 1 µM RHPS4 and (d) 10 µM RHPS4 on KM12 cells between 24 – 96 hours.

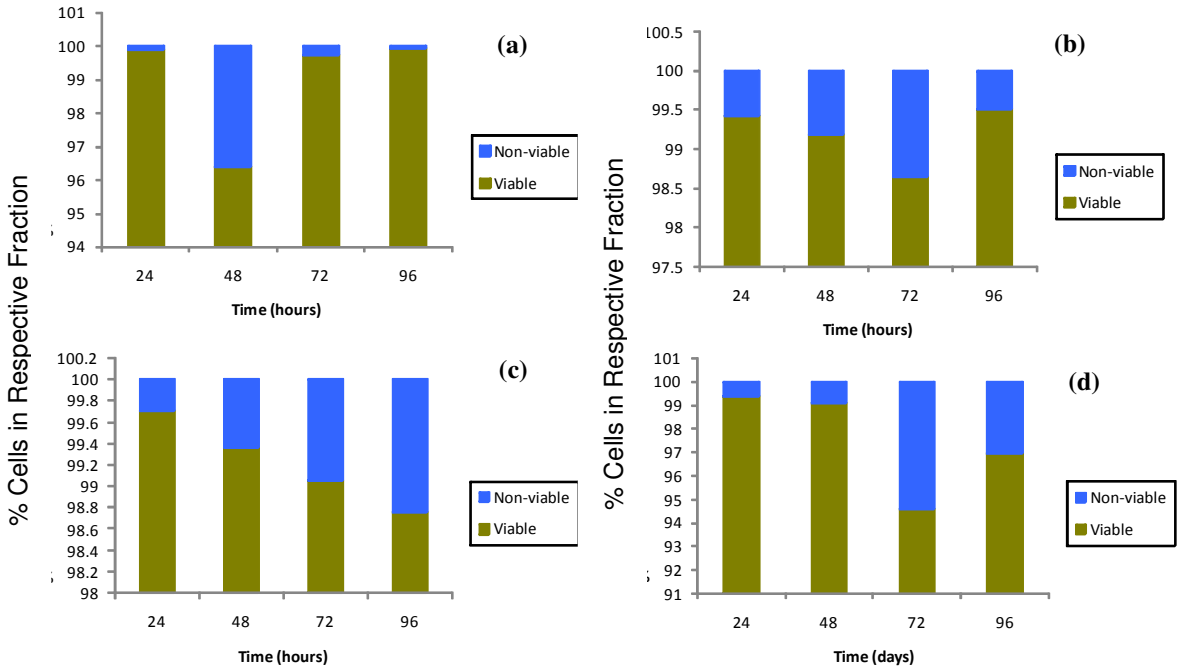


Figure 3.23 Analysis of the new data using the non-viable fraction against the viable fraction estimation. The viable fraction incorporates the cycling cells, i.e. those in G_1/G_0, S and G_2/M, whilst the non-viable fraction incorporates the pre-G_1 fraction. The results shown here depict the effects of (a) control, (b) 100 nM RHPS4, (c) 1 µM RHPS4 and (d) 10 µM RHPS4 on KM12 cells between 24 – 96 hours.

3.4 Ki-67 and Histone H3 as a Marker of G_0 and Mitosis, respectively

The aim of investigating Ki-67 and Histone H3 as markers for G_0 and mitosis, respectively, was to improve the accuracy of the analysis of the effects of RHPS4 on the cell cycle. The method described by Nicolette allows the analysis of the cell cycle using PI, which penetrates the nucleus and intercalates with DNA. Analysis of cell samples stained with PI using a flow cytometry allow the phases of the cell cycle to be distinguished based on DNA content (Nicoletti *et al*, 1991). Cells which are in mitosis have double the amount of DNA of cells in G_1 or G_0 and cells in S phase will have varying amounts of DNA due to them undergoing synthesis. This method is fine; however, it is impossible to distinguish between cells that are in G_2 and M or between cells in G_1 and G_0. By staining the cells with antibodies for proteins only present during the cell cycle in specific phases, the hope is to distinguish between cells in G_1 and G_0, and between cells in G_2 and M.

The expression of the human Ki-67 protein is strictly associated with cellular proliferation and it is during interphone which the antigen can be exclusively detected within the nucleus, whereas during mitosis, the majority of the protein has relocated and can be found on the surfaces of the chromosomes. Manipulation of the fact that this protein is present during all active phases of the cell cycle (i.e. G_1, S and G_2 and M), but is absent from non-proliferating or 'resting' cells (i.e. G_0) makes it an excellent marker for determining the growth fraction of a population of cells (Scholzen & Gerdes, 2000).

Histone H3 is specifically phosphorylated during mitosis in patterns that are specifically coordinated in both space and time (Hans & Dimitrov, 2001). During G_2 to mitosis, the relaxed chromatin is converted into mitotic condensed chromosomes via a process which is considered to be essential for the following nuclear division to correctly separate parental genetic information into two daughter cells. Studies have shown that H3 phosphorylation level is negligible during interphase and reached maximum during mitosis in mammalian cells, making it a good biomarker for detecting the mitotic proportion in a population of cells (Goto *et al,* 1999).

The ease of analyzing the proportion of cells in G_0 and mitosis using Ki-67 and histone H3, respectively were investigated in HT-29 cells as described in section 2.2.7.4. The Ki-67 biomarker is capable of highlighting the proportion of proliferating cells and so there is a shift in the fluorescence of this proportion on the flow cytometry and for the histone H3 there is a shift in the mitotic population. Typical scatter graphs of the Ki-67 and histone H3 fluorescence are shown in figure 3.24. Disappointingly, neither method gives clear results. As stated previously, the proportion of proliferating cells should be clearly highlighted and separate from the proportion of cells in G_0 on the scatter graph produced by the flow cytometer. The results show that in fact there is no clear shift of any proportion of cells within the population of cells though there appears to be a slight shift in a small proportion of cells which may correspond with the mitotic population though cannot be proven. This reduced confidence in this method for analysing the proportion of cells in G_0. The histone H3 stain is used to highlight

the proportion of cells in mitosis from the rest of the cell cycle, including G_2, however, as opposed to shifting the proportion of cells that are not in this phase, the histone H3 stain highlights and shifts the proportion of cells that are in this phase. Disappointingly, the results from this stain were also not of a high standard. The stain was predicting that between 1-3% of cells were in mitosis, which may be true, however, the shift in this small proportion was not as great as would be expected, therefore reducing confidence in this stain also.

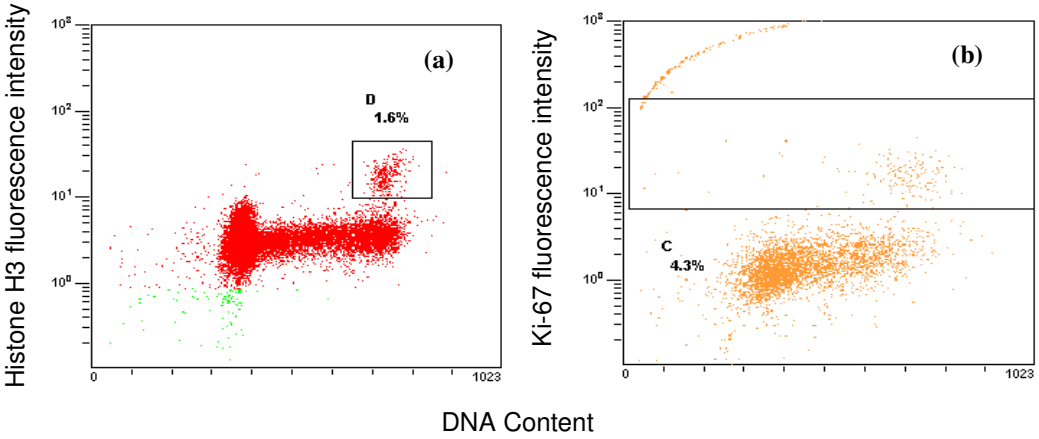


Figure 3.24 Analysis of mitosis and G_0 using antibodies against (a) Histone H3 and (b) Ki-67. Analysis of the cell cycle using PI allows the proportion of cells in each phase of the cell cycle to be analysed, however, does not distinguish between cells in G_1 and G_0 or between cells in G_2 and M. Using an antibody against histone H3 allows the proportion of cells to be distinguished from G_2 as in (a) and using an antibody against Ki-67 allows the proportion of cells in G_0 to be distinguished from the rest of the population of cells as in (b).

To further investigate the accuracy of using an antibody against Histone H3 as a marker of the mitotic population, an experiment using paclitaxel was carried out. Paclitaxel is a mitotic blocker widely used in cancer chemotherapy and was discovered following a series of experiments where it was identified that the proliferation of HeLa cells was inhibited at the nanomolar range (Horwitz, 2004). The theory behind this experiment was that by the addition of serum containing a non-toxic dose of paclitaxel, were we able to visualize the proportion of cells increasing in G_2/M and a parallel increase in the proportion of mitosis as predicted by the histone H3 marker? The cells were incubated with pacliatexel for 18 hours at a concentration of 10 nM, which from earlier experiments was found to be non-

toxic. The cells were then collected as in section 2.2.7.2 and fixed in 75% MeOH. In addition to paclitaxel treated cells, control cells were also analysed that were treated in the same way, however, were not exposed to paclitaxel. The cells were then stained with histone H3 antibody and Ki-67 antibody separately as in chapter 2 and the results are shown in figure 3.25.

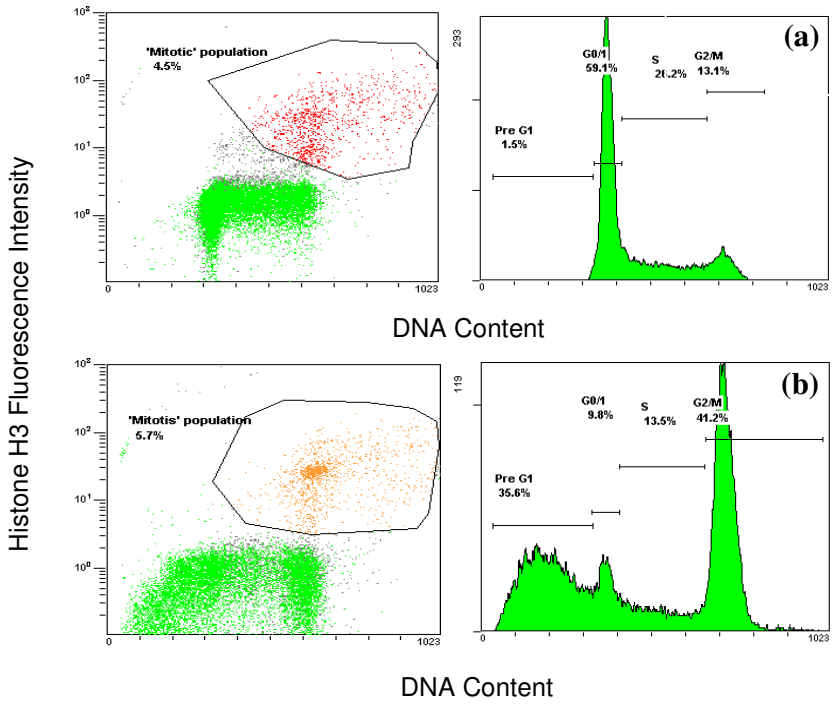


Figure 3.25 Validation of Histone H3 antibody using paclitaxel. To further investigate the use of histone H3 antibody into the analysis of the mitotic population, the cells were incubated in the (a) the absence and (b) the presence of paclitaxel for 18 hours and analysed using an antibody against histone H3, as described in chapter 2.

Figure 3.25 shows the scatter plots for the staining histone H3 in addition to the corresponding cell cycle data. The images clearly show that it is likely that histone H3 antibody is not distinguishing the proportion of mitotic cells at the conditions used. In the absence of paclitaxel, the cell cycle data shows there were 13.1% of cells in the G_2/M phase of the cell whilst the scatter plot suggests that 4.5% of these were in the mitotic phase. The addition of paclitaxel appears to increase the proportion of cells in the G_2/M phase to 41.2% whilst the

corresponding scatter plot suggests that there is only an increase to 5.7% in the proportion of mitotic cells.

3.5 Using BrdU to Determine G_1 to S Kinetics

BrdU is a synthetic nucleoside which is an analogue of thymidine and is incorporated into a cell's DNA when the cell is dividing i.e. during S phase of the cell cycle. Antibodies against BrdU are conjugated to fluorescent markers which can then be used to label and detect these cells and provide visual evidence of cell division on the flow cytometer. When analyzing cell cycle data, the proportion of cells in S phase are easily defined and so BrdU does not increase the accuracy of this estimation. However, the aim was to use BrdU to define the G_1 to S phase kinetics of the cell cycle and therefore increase the amount of data available to apply to the mathematical models. In this investigation, the aim was to incubate the cells with BrdU which would be incorporated in the S phase cells within the population. The cells would then be serum starved and analysed at specific time points to determine the movement of the S phase cells (which have BrdU incorporated in their DNA) through the cell cycle. In doing this we would have a crude estimation of the movement of cells from G_1/G_0 to S phase and define whether only a subpopulation of cells are cycling or are all cells within the population cycling. HCT116 cells were initially used to optimize the protocol and it was found that a lot of optimization was required and this reduced confidence in the assay. A typical scatter plot is shown in figure 3.26 and shows clearly the proportion of cells in G_1/G_0, S and G_2/M. From this scatter plot at different time points, the hope was to trace the movement of cells through the cell cycle, however, as stated previously, the assay required a high level of optimization not only experimentally in terms of antibody concentration, cell number, BrdU concentration etc, but also with respect to limits set on the flow cytometer and therefore reduced confidence in whether we were seeing a true reflection of the actual conditions of the cells.

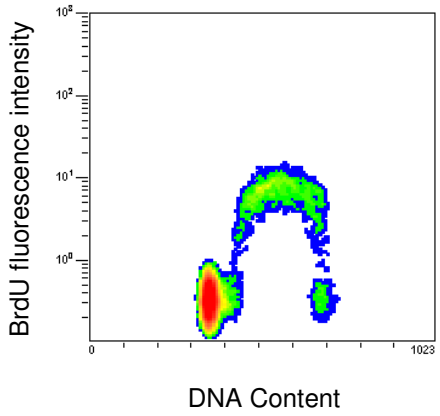


Figure 3.26 Analysis of G_1 to S phase kinetics using BrdU. The cells were stained with BrdU in an attempt to analyse to G_1 to S kinetics in HCT116 cells. The cells were analysed using the flow cytometer whereby 20 000 events were collected.

3.6 Conclusions

The aim of the biological studies was to determine which of the four colorectal cell lines HCT116, HT-29, KM12 and HCC-2998 was the most robust in terms of their growth properties, sensitivity to RHPS4 and their senescence properties under normal conditions and in response to RHPS4. From these studies, a cell line was chosen in order to develop a mathematical model which allowed the data that was generated to be modelled and used to reveal aspects of the mechanism of action of RHPS4 that would be difficult to determine without it. Desirable characteristics from the cell line included:

- Reliability in a range of biological assays.
- Good sensitivity to RHPS4.
- Reliable growth properties to allow senescence and cell cycle analysis.

Based on the results of biological studies, it was decided that the HCT116 cell line would be used to analyse the mechanism of action of RHPS4. Of all the cell lines analysed, they were the most reliable in terms of their growth properties, but also their sensitivity to RHPS4 and their ease of analysis in the SA-β-gal assay to determine senescence.

The HCC-2998 cell line was the most unreliable of the four cell lines. The cell line had the longest doubling time which may affect the analysis of the short-term

effects of RHPS4. In order to determine cell cycle effects, it is necessary that the cells undergo a number of cycles. The HCC-2998 cells had a very long doubling rate hence making analysis of the cell cycle effects more difficult. The KM12 cell line, although the most sensitive to RHPS4, had the least favourable morphology for analysing senescence. Rather than growing in a monolayer like the HCC-2998, HCT116 and HT-29 cell lines, KM12 cells grew in layers and so it was impossible to analyse the proportion of senescent cells in the lower layers, which, obviously, form part of the population. As stated previously, KM12 cells were the most sensitive of the four cell lines tested. Cookson *et al* proposed in 2005 that sensitivity to RHPS4 is related to telomere length. They determined that *mt*-hTERT-transfected MCF-7 cells possessing short telomeres were 10-fold more sensitive to RHPS4. Overall, their study concluded a relationship between shorter telomeres and sensitivity to RHPS4 (Cookson *et al*, 2005). Telomere shortening and telomerase activation occur frequently in cases of colorectal carcinoma. It is possible that the greater sensitivity of KM12 to RHPS4 is due to reduced telomere length in KM12 cells in comparison to the other colorectal cell lines. A study carried out Myung *et al* revealed that the average length of the telomeres in HCT116 cells was in the range of 3 to 9 kb, with an average 5.6±0.8 kb (n=11). The telomere lengths were analysed using the TRF assay which is a well established assay (Myung *et al*, 2004). In comparison to this, another study carried out by Brown *et al* determined that the average length of HT-29 telomeres was 8.9 kb using southern analysis (Brown *et al*, 2003). Although the telomere lengths of the HCC-2998 and KM12 cells could not be found in the literature, a study carried out in 2002 whereby the average telomere lengths of 20 samples of invasive colorectal cell lines were calculated using densitometric analysis of autoradiographs which uses a transmitter scanning video densitometer and was determined to be 7.12±0.14 kb. In the same study, it was also found that the telomere length of the normal colonic mucosa was found to be 9.25±0.16 kb, which is significantly longer than that of carcinoma cell lines (Rok Kim *et al*, 2002). It has been found that the telomere length of HCT116 cells is the shortest, although we are not sure of the exact telomeric lengths of KM12 or HCC-2998. If

the theory of Cookson *et al* is true, whereby it there is a link between shorter telomeres and increased sensitivity to RHPS4 in MCF-7 cells, this would suggest that HCT116 cells would be more sensitive to the action of RHPS4 than HT-29 cells. In the study carried out we identified that it was in fact the KM12 cell line that displayed the greatest sensitivity to RHPS4 and therefore concluding that maybe the sensitivity of these colorectal cell lines cannot be explained by telomere lengths alone.

In order to determine sensitivity to RHPS4, GI_{50} values for each cell line was determined at 24 hours and 72 hours. To reiterate, a GI_{50} value is the concentration of an agent to cause 50% growth inhibition. MTT assays of HCT116, HT-29, KM12 and HCC-2998 in the presence of a range of concentrations of RHPS4 show that the GI_{50} of KM12 and HCC-2998 increase (non-significantly) from 24 to 72 hours therefore suggesting there is a decrease in sensitivity and could be due to the increased resistance of the cells to the effects of RHPS4. The opposite is true for HCT116 and HT-29 cells whose GI_{50} values actually decrease, though again non-significantly, therefore suggesting increased sensitivity of these cell lines to RHPS4. The underlying mechanism for the different responses is unknown.

Appendix III shows the NCI 60-cell line panel data for RHPS4. The 60-cell line panel is a series of human tumour cell lines which have been specifically chosen to represent nine different tumour types and used to carry out a large *in vitro* screening program for novel anti-cancer agents. Up until 2001, more than 60 000 different compounds have been characterized using this screen with respect to their anti-tumour activity and amongst them has been RHPS4 (Yu *et al*, 2001). The NCI 60-cell line panel found that for RHPS4, the corresponding GI_{50} values for HCT116, HT-29, KM12 and HCC-2998 were 19.9 µM, 33.1 µM, 4.7 µM and 3.9 µM, respectively. The data suggests that the most sensitive cell line is the KM12 cell line, and is parallel with what we found in the present study.

The changes in response to RHPS4 between the short and longer term experiments could be explained in terms of p53 status. It is also important to note that the HCT116 cell line is the only cell line of the four chosen for initial study to have

p53 wild-type status. The p53 protein functions as a tumour suppressor gene and also acts as an integrator of upstream signals and then acts as a central node in a signal transduction network which responds to minimize mutations and other errors which can lead to cancers (Levine *et al*, 2004). Studies carried out by Finlay *et al* in 1989 using transformed clones suggested that the p53 wild-type gene was acting like an anti-oncogene tumour suppressor gene. In the same experiments, the data was also indicative of p53 mutant cell lines had lost their tumour suppressor activity and could explain the changes that occur between the short and longer term experiments.

The HT-29 cell line was very similar to the HCT116, in terms of morphology, doubling time and sensitivity to RHPS4; however, was slightly less reliable in the Nicoletti assay for determining cell cycle, particularly when analysing the short-term effects of RHPS4.

HCT116 cells were chosen for further study and the development of mathematical models in order to give us a preliminary insight into the mode of action of RHPS4 and other anti-tumour agents. It was determined that the morphology of HCT116 cells was the most favourable as they made senescence analysis easy. Without incorporating senescence data into the mathematical models, a major component of the cell cycle would be omitted and may affect any conclusions. Not only was their morphology favourable, but also their doubling rate and tractability in cell cycle analysis and other biological assays.

Also highlighted in this chapter is the need for data of a higher quality and confidence in the method of analysis. Systems biology is the analysis of the relationships among the elements of a system in response to either genetic or environmental perturbations with the goal being the understanding of the system and its emergent properties. Systems biology is hypothesis-driven as we begin with a model that is tested with hypotheses that require systems perturbations (Weston & Hood, 2004). In this study, we have a model of the cell cycle as outline in chapter 4 that is tested with data sets in chapter 5 to probe the mechanism of action of RHPS4. To have confidence in the conclusions of the model, the data sets need to be robust and of a high quality. In this chapter, we

explore the methods available for the analysis of the pre-G_1 fraction. It appears that the least favourable is the analysis of the cell cycle in terms of viable versus non-viable.

The validity of the mathematical model and simulations is based on the robustness of the experimental data. Cell cycle analysis using DNA content to 'compartmentalise' sub-cellular fractions offers a statistically robust method, however, the extraction of parameters can be implemented by different methods. This chapter attempts to determine both the robustness of the analysis for objective parameterisation and confidence in the analysis. As shown by many previous cell cycle cytometrists systematic gating and the reporting of those gates offers a consistent approach. The next generation of flow cytometry analysis particularly data for publication and data for repositories will require compliance with the new evolving data standard MiFlowCyt. In the current study the conservative approach to estimate the pre-G_1 fraction is on the basis of DNA fluorescence intensity and that is the basis on which the model simulations will be conducted (Lee *et al*, 2008). To improve this analysis in future experiments, would involved better estimates of cell death and apoptosis by splitting the samples each time and performing parallel cell cycle and Annexin V analysis.